Knockdown of PHOX2B in the retrotrapezoid nucleus reduces the central CO_2 chemoreflex in rats.

Silvia Cardani [*1,2], Tara A. Janes [*1,2], William Betzner[1§], Silvia Pagliardini[#1,2,3]

[1]Department of Physiology, Faculty of Medicine and Dentistry, University of Alberta, Edmonton AB T6G2E1 Canada,

[2]Women and Children's Health Research Institute, University of Alberta, Edmonton AB T6G2E1 Canada.

[3]Neuroscience and Mental Health Institute, University of Alberta, Edmonton AB T6G2E1 Canada.

*SC and TAJ contributed equally to this work

[§] Current address: Departments of Clinical Neurosciences and Community Health Sciences, Hotchkiss Brain Institute, University of Calgary Cumming School of Medicine, Calgary AB T2N 4N1

[#]Corresponding author: Silvia Pagliardini, Department of Physiology, Faculty of Medicine & Dentistry, University of Alberta, 3020F Katz Group- Rexall Centre

Email: silviap@ualberta.ca.

Acknowledgments/ Author contributions

Concept and experimental design, S.P. and S.C.; Data collection, S.C., W.B. and S.P.; Data analysis, S.C. and T.A.J.; Manuscript preparation, S.C., T.A.J. and S.P.

S.C. is supported by the Canadian Lung Association BaO Fellowship. T.A.J. is supported by the Canadian Institutes for Health Research (CIHR) Postdoctoral Fellowships. S.P. is supported by a Women and Children's Health Research Institute Innovation Grant and CIHR Project scheme grant.

ABSTRACT

PHOX2B is a transcription factor essential for the development of different classes of neurons in the central and peripheral nervous system. Heterozygous mutations in the PHOX2B coding region are responsible for the occurrence of Congenital Central Hypoventilation Syndrome (CCHS), a rare neurological disorder characterised by inadequate chemosensitivity and life-threatening sleep-related hypoventilation. Animal studies suggest that chemoreflex defects are caused in part by the improper development or function of PHOX2B expressing neurons in the retrotrapezoid nucleus (RTN), a central hub for CO_2 chemosensitivity.

Although the function of PHOX2B in rodents during development is well established, its role in the adult respiratory network remains unknown. In this study, we investigated whether reduction in PHOX2B expression in chemosensitive neuromedin-B (NMB) expressing neurons in the RTN altered respiratory function. Four weeks following local RTN injection of a lentiviral vector expressing the short hairpin RNA (shRNA) targeting *Phox2b* mRNA, a reduction of PHOX2B expression was observed in *Nmb* neurons compared to both naïve rats and rats injected with the non-target shRNA. PHOX2B knockdown did not affect breathing in room air or under hypoxia, but ventilation was significantly impaired during hypercapnia. PHOX2B knockdown did not alter *Nmb* expression but it was associated with reduced the expression of both *Task2* and *Gpr4*, two CO_2 sensors in the RTN. We conclude that PHOX2B in the adult brain has an important role in CO_2 chemoreception and reduced PHOX2B expression in CCHS beyond the developmental period may contribute to the impaired central chemoreflex function.

INTRODUCTION

The Paired Like Homeobox 2B (PHOX2B) is a transcription factor essential for embryonic differentiation and for the maintenance of the neuronal phenotype of different classes of neurons in both the central and peripheral nervous systems (Brunet & Pattyn, 2002; Pattyn et al., 1997, 1999, 2000; Stanke et al., 1999; Tiveron et al., 1996). In recent years, the PHOX2B gene has been extensively investigated, not only for its neurodevelopmental role, but also because its heterozygous mutation leads to Congenital Central Hypoventilation Syndrome (CCHS, OMIM 209880; Amiel et al., 2003), Hirschsprung's disease (HSCR; OMIM 142623; Berry-Kravis et al., 2006; Trochet et al., 2005), and neuroblastoma (Bourdeaut et al., 2005; Van Limpt et al., 2004). CCHS is a rare (1:200,000 births in France (Trang et al., 2005) and 1:148,000 births in Japan (Shimokaze et al., 2015) disorder characterised by a failure to respond to both hypercapnia and hypoxia (Amiel et al., 2003; Di Lascio et al., 2021; Weese-Mayer et al., 2017). The most frequent PHOX2B mutation is an expansion of a polyalanine repeat, ranging from +5 to +13 residues on the C-terminal of PHOX2B, an area that regulates DNA binding affinity and protein solubility (Amiel et al., 2003; Di Lascio et al., 2016; Weese-Mayer et al., 2003). CCHS symptoms present with varying degrees of severity depending on the expansion of the mutation (Berry-Kravis et al., 2006; Di Lascio et al., 2018; Matera, 2004). In most mild cases, patients display normal ventilation during wakefulness, hypoventilation during sleep leading to hypercarbia and hypoxemia, as well as a lack of sensitivity and discomfort to these challenges. In the most severe of cases, hypoventilation may also be present while awake.

Respiratory disturbances resulting from the PHOX2B mutations appear to stem from its widespread expression in respiratory-related neurons both during development and into adulthood. Although PHOX2B is absent in respiratory rhythmogenic neurons of the preBötzinger

complex, it is highly expressed in adult neurons that are responsible for CO_2 and O_2 chemoreflexes (Kang et al., 2007). Among those are the neurons of the retrotrapezoid nucleus (RTN), the locus coeruleus, the carotid bodies and the nucleus of the solitary tract that, together with the dorsal motor nucleus of the vagus nerve and the area postrema, make up to the dorsal vagal complex, a structure that provides the major integrative centre for the mammalian autonomic nervous system (Cutsforth-Gregory & Benarroch, 2017; Guyenet et al., 2019; Kang et al., 2007; Zoccal et al., 2014). Previous work by our group and others specifically investigated the role of PHOX2B-expressing RTN neurons by either selective lesions or inactivation of neuronal activity of these neurons (Abbott et al., 2011; Basting et al., 2015; Marina et al., 2010; Nattie & Li, 1994; Souza et al., 2018, 2023; Janes et al., 2024) and showed that RTN neurons have a key role in central CO_2 chemoreception.

Defects observed in the CO_2-chemoreflex of CCHS transgenic rodent models are primarily caused by the improper development or function of PHOX2B-expressing neurons in the RTN (Dubreuil et al., 2008; Ramanantsoa et al., 2011), although anatomo-pathological studies in CCHS patients suggest that the respiratory impairment may be caused by a more widespread brain dysfunction (Harper et al., 2015; Nobuta et al., 2015). Transgenic mice born with PHOX2B knockout fail to develop the RTN, the locus coeruleus (Pattyn et al., 1999) and catecholaminergic groups in A1, A2, A5 and A7 (Pattyn et al., 2000), as well as neurons of the nucleus of the solitary tract and the carotid bodies. Mice harbouring heterozygous PHOX2B knockout develop apparently normal but have depressed responses to hypoxia and hypercapnia (Dauger, 2003) and sleep disordered breathing in the perinatal period (Durand et al., 2005). Furthermore, the expression of the most common heterozygous PHOX2B mutation found in CCHS patients (PHOX2B +7Ala expansion) in mice results in a near complete loss of RTN neurons, impaired CO_2 response and consequent death

97 in the newborn period (Dubreuil et al., 2008; Madani et al., 2021; Ramanantsoa et al., 2011;
98 Takakura et al., 2008). More selective expression of the mutant PHOX2B in the RTN neurons
99 allowed for survival in the neonatal period and partial recovery of the CO_2 response in adulthood
100 (Ramanantsoa et al., 2011).
101
102 Multiple potential cellular mechanisms have been implicated in the aetiology of CCHS, from loss of
103 PHOX2B function in development due to heterozygous mutant PHOX2B expression, to gain of
104 function of the mutated protein that may alter transcriptional activity in neurons, as well as
105 aggregate formation and premature cell death (Bachetti et al., 2005; Di Lascio et al., 2013;
106 Dubreuil et al., 2008; Durand et al., 2005; Goridis et al., 2010; Trochet et al., 2005). While its role
107 during embryonic neurodevelopment is established, PHOX2B is still expressed in selected neuronal
108 populations in the adult brain (Kang et al., 2007; Stornetta et al., 2006) and its function, with the
109 exception of the contribution to the maintenance of the noradrenergic phenotype (Fan et al.,
110 2011), is not yet fully understood. Considering the fundamental role of PHOX2B in CCHS
111 pathogenesis and its expression in key structures for CO_2 chemoreflex responses, it is essential to
112 understand how both wild-type and mutant PHOX2B proteins impact CO_2 homeostasis and
113 ventilation not only across development, but also in adulthood.
114 In order to have a better understanding of the role of PHOX2B in the CO_2 homeostatic processes
115 we used a non-replicating lentivirus vector of two short-hairpin RNA (shRNA) clones targeting
116 selectively *Phox2b* mRNA to knockdown the expression of PHOX2B in the RTN of adult rats and
117 tested ventilation and chemoreflex responses. In parallel, we also determined whether
118 knockdown of PHOX2B in adult *Nmb* neurons of the RTN negatively affected their cell survival.
119 Finally, we sought to provide a mechanistic link between PHOX2B expression and the
120 chemosensitive properties of *Nmb* neurons of the RTN, which have been attributed to two proton

121 sensors, the proton-activated G protein-coupled receptor (GPR4) and the proton-modulated
122 potassium channel (TASK-2) (Gestreau et al., 2010; Guyenet et al., 2016; Kumar et al., 2015). The
123 expression of these sensors is partially overlapping in *Nmb* neurons of the RTN and the genetic
124 deletion of either one impairs the central respiratory chemoreflex with maximal impairment when
125 both sensors are eliminated (Gestreau et al., 2010; Guyenet et al., 2016; Kumar et al., 2015).
126 Our results indicate that progressive knockdown of PHOX2B in RTN causes a reduction in the
127 chemoreflex response that was proportional to the decrease in the fraction of *Nmb*/PHOX2B
128 expressing RTN neurons. This effect was associated with a reduction in the expression of *Gpr4* and
129 *Task2* mRNA in *Nmb* expressing cells of the RTN in which PHOX2B was knocked down, suggesting a
130 role for PHOX2B in the transcription of the proton sensors in RTN neurons.
131

132 **RESULTS**

133

134 To directly investigate the role of PHOX2B in RTN neurons, we performed selective knockdown of
135 this protein in adult rats through local injection of a non-replicating lentiviral vector of two short-
136 hairpin RNA (shRNA) clones targeting two different sequences of the *Phox2b* mRNA (n=25) or non-
137 target shRNA as control (NT-shRNA; n=23). Initial experiments utilized 200 nl/injection at each of 4
138 stereotaxic coordinates ($1x10^9$ VP/ml; n=14). Four weeks post injection, we assessed ventilatory
139 parameters in room air, hypercapnia, and hypoxia. Interestingly, a small but significant impairment
140 in the CO_2 chemoreflex was observed not only in PHOX2B-shRNA but also in NT-shRNA rats
141 compared to pre-surgical baseline (allometric V_E in 7% CO_2: -21% and -24%, respectively; Supp. Fig.
142 1A). Because histological analysis also showed significant reduction of Nmb^+/PHOX2B$^+$ RTN cells in
143 NT-shRNA and PHOX2B-shRNA rats (33% and 19% cells remaining, respectively; Suppl. Fig. 1), we

144 concluded that the volume and titre of the shRNA viral constructs triggered off-target effects
145 (Mcbride et al., 2008; Van Gestel et al., 2014) that cause cell death in RTN neurons.

146

147 **PHOX2B expression is modestly reduced two weeks following infection without respiratory**
148 **impairment.**

149 Due to the off-target effects obtained with large volume injections, we reduced injection volume
150 of both PHOX2B shRNA (n=17) and NT-shRNA viruses (n=17) (4x100nl/injection; $1x10^9$ VP/ml).

151 Two weeks post-surgery we assessed respiratory function during exposure to room air,
152 hypercapnia and hypoxia. Overall, we observed little change in respiration at this time point.
153 During room air, as well as in 5% and 7.2% CO_2, frequency (f_R), was reduced in every experimental
154 group (naïve, NT-shRNA, PHOX2B-shRNA) compared to baseline (Air: $p=0.014$; 5% CO_2: $p< 0.001$;
155 7.2% CO_2 $p< 0.001$; Fig. 1A) but no effect on treatment was observed, suggesting that these
156 changes were likely due to the increase in age and body weight during the long-term experiment
157 (naïve: +32.2%; NT-shRNA: +27.8%; PHOX2B-shRNA: +28.6% change in body weight). Tidal volume
158 was reduced in the PHOX2B-shRNA rats at 7.2% CO_2 compared to both naïve rats (naive: 9.6 ± 1.2
159 $ml{\cdot}kg^{-1}$; PHOX2B-shRNA: 8.5 ± 0.9 $ml{\cdot}kg^{-1}$; -11%; $p= 0.022$) and baseline pre-surgery conditions
160 (baseline: 9.6 ± 1.3 $ml{\cdot}kg^{-1}$; -11%; $p< 0.001$; Fig. 1B) but it was not different from NT-shRNA.

161 Despite similar changes in body weight across treatment groups, allometric ventilation (V_E ALLO)
162 was higher in naïve rats compared to the other treatment groups in room air (naïve: 38.4 ± 4.5
163 $ml{\cdot}min^{-1}$; NT-shRNA: 34.7 ± 2.8 $ml{\cdot}min^{-1}$; PHOX2B-shRNA: 34.0 ± 4.5 $ml{\cdot}min^{-1}$; $p=0.005$; Fig. 1C), but
164 no changes in V_E ALLO were observed in hypercapnia (7.2% CO_2) across treatments (naïve : 91.5 ±
165 13.2 $ml{\cdot}min^{-1}$; NT-shRNA: 84.4 ± 13.7 $ml{\cdot}min^{-1}$; PHOX2B-shRNA: 80.5 ± 17.2 $ml{\cdot}min^{-1}$). Oxygen
166 consumption (VO_2 ALLO) was not different between experimental conditions or treatment groups

167 (Fig. 1D), and V_E/VO_2 ALLO indicated that ventilation was matched with metabolism for each
168 treatment across all gas compositions (naïve: 7.7 ± 1.3; NT-shRNA: 7.2 ± 1.3; PHOX2B-shRNA: 6.9 ±
169 2.0; Fig. 1E). These results suggest that despite a reduction in hypercapnic V_T in the PHOX2B-
170 shRNA rats, overall ventilation was not impaired. Since we observed differences in room air V_E
171 ALLO between treatment groups, we normalized these data to show the hypercapnic ventilatory
172 response (HCVR, i.e., absolute change in V_E from room air; Fig. 1F). The HCVR was also not affected
173 by the PHOX2B shRNA treatment two weeks post-injection (naïve: 53.1 ± 13.4 $ml{\cdot}min^{-1}$; NT-shRNA:
174 49.6 ± 13.2 $ml{\cdot}min^{-1}$; PHOX2B-shRNA: 46.5 ± 14.8 $ml{\cdot}min^{-1}$).

175 To determine the extent of PHOX2B knockdown in RTN neurons we combined RNAScope® and
176 immunohistochemistry assays to quantify RTN neurons expressing *Nmb* and PHOX2B (Fig. 2B). We
177 reasoned that by assessing the fraction of RTN neurons that express only *Nmb* (compared to
178 *Nmb*$^+$/PHOX2B$^+$), we would be able to determine the level of PHOX2B knockdown in our
179 experiments. Two weeks post viral injection, we observed a small decrease (15.2%) in the total
180 number of *Nmb* RTN neurons (i.e., *Nmb*$^+$/PHOX2B$^+$ plus *Nmb*$^+$/ PHOX2B$^-$) in NT-shRNA rats
181 compared to naïve rats (naïve; 337.6 ± 11.95; n=4; NT-shRNA: 286.0 ± 10.44; n=4; $p<0.001$; Fig.
182 2C). The total number of *Nmb* cells of the RTN in PHOX2B-shRNA rats was further reduced
183 compared to both naïve rats (PHOX2B-ShRNA 218.8 ± 7.8 n=4; -35.2%; $p<0.001$) and to NT-shRNA
184 (-23.5%; $p<0.001$).

185 We then quantified the number of neurons in the RTN expressing either *Nmb* and PHOX2B
186 (*Nmb*$^+$/PHOX2B$^+$) or *Nmb* only (*Nmb*$^+$/PHOX2B$^-$). The number of *Nmb*$^+$/PHOX2B$^+$ neurons in
187 PHOX2B-shRNA rat was reduced by 36.1 % compared to NT-shRNA and by 46.2% compared to
188 naïve rats (*Nmb*$^+$/PHOX2B$^+$ NT-shRNA: 232.3 ± 11.6 vs naïve: 275.8 ± 17.1; vs PHOX2B-shRNA:
189 148.3 ± 12.6; $p<0.05$ and 0.001, respectively; Fig. 2C,D). On the contrary, the fraction of
190 *Nmb*$^+$/PHOX2B$^-$ neurons in PHOX2B-shRNA rat was not different compared to naïve and NT-shRNA

191 rats (*Nmb*$^+$/PHOX2B$^-$ NT-shRNA: 53.7 +- 8.6; vs naïve: 61.8 +-13.9; vs PHOX2B-shRNA: 70.5 +- 8.7
192 cells; Fig. 2C,E). These results thus indicate that despite modest loss of *Nmb*$^+$ neurons in NT-shRNA
193 and a reduction in the proportion of *Nmb* neurons expressing PHOX2B in PHOX2B-shRNA rats, 2
194 weeks of PHOX2B shRNA viral infection was not sufficient to impair ventilation.

195 **Four weeks of PHOX2B knockdown impairs the CO_2-chemoreflex.**

196 Since the shRNAs integrate into the genome of the infected cells and are continuously produced, it
197 is reasonable to expect that knockdown efficiency is time-dependent, and an extended infection
198 time would result in a higher knockdown effect. To test this hypothesis, a subgroup of rats (naïve,
199 NT-shRNA and PHOX2B-shRNA) were investigated four weeks post-viral injection (Fig. 3A,B).

200 The total number of *Nmb* neurons in the RTN of PHOX2B-shRNA rats (*Nmb*$^+$/PHOX2B$^+$ plus
201 *Nmb*$^+$/PHOX2B$^-$; Fig. 3C) was significantly reduced compared to naïve rats (naïve: 347.8 ± 12 cells,
202 n=4; PHOX2B-shRNA: 249.5 ± 33.9 cells; n=6; -28.3%; p=0.009) but no difference was observed
203 compared to NT-shRNA rats (294.9 ± 52.8 cells; n=10; -15.4%;). Furthermore, there was no
204 difference in the total number of *Nmb* cells in RTN between 2 and 4 weeks post infection for both
205 NT-shRNA (week 2: 286 ± 10.4; week 4: 294.9 ± 52.8, p=0.783) and PHOX2B-shRNA rats (week 2:
206 218.8 ± 7.8; week 4: 249.5 ± 33,9, p=0.118), suggesting that the progressive PHOX2B knockdown
207 was specific for PHOX2B-shRNA treatment and it was not accompanied by an increased cell death
208 beyond the first 2 weeks.

209 The number of *Nmb*$^+$/PHOX2B$^+$ cells in the RTN was significantly reduced in PHOX2B-shRNA rats by
210 67.0% and 60.7% compared to naïve and NT-shRNA rats, respectively (naïve: 284.5 ± 19.8; NT-
211 shRNA: 238.7 ± 56; PHOX2B-shRNA: 93.8± 11.9 cells, p<0.001; Fig. 3D). Moreover, a significant
212 increase in the fraction of *Nmb*$^+$/PHOX2B$^-$ was observed with PHOX2B knockdown (PHOX2B-
213 shRNA: 155.7 ± 22.7; naïve: 63.2 ± 12cells; + 146.1% increase vs naïve; NT-shRNA: 56.2 ± 13.8cells;

214 + 177% increase vs NT-shRNA, p<0.001; Fig. 3E), confirming the efficiency of the PHOX2B
215 knockdown in the *Nmb* cells of the RTN.

216 The respiratory function prior to histological examination (4 weeks post-viral injection) showed
217 significant differences in PHOX2B-shRNA rats (n=6) compared to both pre-surgery baseline, naïve
218 (n=8) and NT-shRNA rats (n=10). Similar to what we reported at 2 weeks post-surgery, f_R at 4
219 weeks was lower in every treatment group compared to baseline recordings (Air: p=0.001; 5% CO_2:
220 p< 0.001; 7.2% CO_2 p< 0.001; Fig. 4A).

221 During room air, V_T was reduced in naïve rats compared to baseline (baseline: 5.9 ± 0.5 ml·kg^{-1};
222 week 4: 5.2 ± 0.6 ml·kg$^{-1;}$ -12%; p=0.001; Fig. 4B). Moreover, V_T in PHOX2B-shRNA rats was reduced
223 compared to NT-shRNA (NT-shRNA: 5.6 ± 0.4 ml·kg^{-1}; PHOX2B-shRNA: 5.3 ± 0.4 ml·kg^{-1}; -10%;
224 p=0.043) and to the pre-surgery baseline (6.1 ± 0.7 ml·kg^{-1}; -18%; p=0.002). No significant changes
225 were observed at 5% CO_2, although a decrease in V_T occurred at 7.2% CO_2 in PHOX2B-shRNA rats
226 compared to pre-surgery baseline (baseline: 7.7 ± 1.2 ml·kg^{-1}; PHOX2B-shRNA: 6.7 ± 0.6 ml·kg^{-1}; -
227 31%; p<0.001), naïve rats (7.9 ± 0.9 ml·kg^{-1}; -26%; p<0.001), and NT-shRNA rats (8.1 ± 0.7 ml·kg^{-1}; -
228 23%; p=0.002).

229 Decreased V_T observed for PHOX2B-shRNA led to a ventilation (V_E ALLO) impairment during
230 exposure to hypercapnia (7.2% CO_2, PHOX2B-shRNA vs. NT-shRNA: -17%; p=0.021; PHOX2B-shRNA
231 vs. naïve; -21%; p=0.007; PHOX2B-shRNA vs. baseline, -18% p=0.002; Fig. 4C). Since O_2-
232 consumption (VO_2 ALLO) did not change (data not shown) a significant reduction in V_E/VO_2 ALLO
233 confirmed alveolar hypoventilation in PHOX2B-shRNA animals compared to NT-shRNA rats both at
234 5% (NT-shRNA: 5.8 ± 0.5; PHOX2B-shRNA: 4.8 ± 0.4; -16%; p=0.023) and 7.2% CO_2 (NT-shRNA: 7.9 ±
235 1.2; PHOX2B-shRNA: 6.1 ± 0.8; -24%; p=0.004; Fig. 4D). Moreover, the HCVR (Fig. 4E) at 7.2% CO_2
236 was lower in PHOX2B-shRNA (40.3 ± 9.4 ml·min^{-1}) rats compared to the pre-surgery baseline (58.1
237 ± 8.9 ml·min^{-1}; -31%; p=0.015), naïve rats (63.6 ± 14.3 ml·min^{-1}; -37%; p=0.008) and NT-shRNA rats

238 (56.0 ± 10.4 ml·min^{-1}; -28%; p=0.016). Analysis of individual rats in each treatment group over
239 time showed that the HCVR was only consistently impaired in PHOX2B-shRNA rats between weeks
240 2 and 4 (Fig. 1F; p=0.007).
241 Given that previous studies have proposed a role for the RTN in the hypoxic chemoreflex (Barna et
242 al., 2016; Basting et al., 2015; Gourine et al., 2005; Wickström et al., 2004), and we observed
243 impairment of the CO_2-chemoreflex at 4 weeks post-infection, we investigated whether PHOX2B
244 knockdown would also affect respiratory response to hypoxia (10% O_2). The 4 week V_E ALLO was
245 increased relative to baseline values in naïve (baseline: 62.3 ± 5.2 ml·min^{-1}; naïve: 71.0 ± 10.1
246 ml·min^{-1}; +14%), NT-shRNA (baseline: 71.8 ± 11.1 ml·min^{-1}; NT-shRNA: 75.8 ± 12.8 ml·min^{-1}; +6%)
247 and PHOX2B-shRNA rats (baseline: 65.9 ± 9.8 ml·min^{-1}; PHOX2B-shRNA: 79.3 ± 6.4 ml·min^{-1}; +29%;
248 p<0.001). However, analysis of the convective requirement ratio (V_E/VO_2 ALLO) indicates that
249 changes in hypoxic ventilation were due to metabolic adjustments that occurred in all treatment
250 groups (VE/VO_2 ALLO naive: 6.5 ± 1.3; NT-shRNA: 6.7 ± 1.7; PHOX2B-shRNA: 6.6 ± 0.6), suggesting
251 that the hypoxic ventilatory response was not affected by PHOX2B knockdown.

252

253 **PHOX2B knockdown does not extend to C1 catecholaminergic neurons and does not affect**
254 **mRNA expression of *Nmb* in RTN neurons**

255 To exclude that the observed chemoreflex impairment was due to unintended knockdown of
256 PHOX2B in adjacent areas of the brain, we quantified the total number of TH^+/PHOX2B$^+$
257 catecholaminergic C1 neurons in PHOX2B-shRNA rats compared to naïve and NT-shRNA (Fig.
258 5A,B). No differences were observed in either the TH^+ cell numbers or in the TH^+/PHOX2B$^+$
259 neurons between the 3 treatment groups (TH^+/PHOX2B$^+$ cells: naïve: 378.3 ± 23.81; NT-shRNA:
260 391.7 ± 33.08; PHOX2B-shRNA: 370.2 ± 33.04 cells) (Fig. 5B).

261 Neuromedin B is currently considered the most selective anatomical marker for chemosensitive
262 RTN neurons (Shi et al., 2017) and was used in this study to identify RTN location, cell numbers
263 and relative PHOX2B expression. Since changes in the level of the transcription factor PHOX2B
264 could regulate the expression of its target genes, we investigated whether *Nmb* is a target gene of
265 PHOX2B and it is affected by PHOX2B knockdown. We assessed *Nmb* expression in individual RTN
266 cells of PHOX2B-shRNA rats and compared its cellular expression to both naïve and NT-shRNA rats
267 (Fig 5B). Neuromedin B mRNA expression was calculated as total fluorescence intensity (CTCF)
268 ratio in single cells of the RTN relative to the single cell *Nmb* expression measured at the level of
269 NTS *Nmb* cells, which served as an internal control (Fig. 5D). We observed no changes in relative
270 fluorescence of *Nmb* in RTN neurons across the 3 groups (p=0.608), suggesting that *Nmb* levels in
271 RTN neurons are not affected by PHOX2B knockdown.

272 To better analyse the effect of PHOX2B knockdown on the attenuation of the HCVR, we evaluated
273 the correlation between the number of Nmb^+/$PHOX2B^+$ or Nmb^+/$PHOX2B^-$ cells in the RTN and the
274 resulting HCVR using linear regression (Fig. 5E,F). Our results indicate that there is a significant
275 correlation between HCVR and number of Nmb^+/$PHOX2B^+$ ($r^2 = 0.739$ $p<0.001$; Fig. 5E), and
276 Nmb^+/$PHOX2B^-$ ($r^2 = 0.482$ $p<0.001$ Fig. 5F) cells, suggesting that the number of PHOX2B expressing
277 cells in the RTN is a good predictor of the chemoreflex response. Moreover, the nature of the
278 correlation between $PHOX2B^-$ cells and HCVR is the opposite of $PHOX2B^+$, another important
279 indicator that PHOX2B protein may contribute to the CO_2 sensing and consequently, the reduction
280 of PHOX2B protein impairs the CO_2-chemoreflex.

281

282 **Gpr4 and Task2 mRNAs expression is affected by PHOX2B Knockdown**

283 We next examined the mRNA expression of *Gpr4* and *Task2*, two important pH sensors for the
284 central respiratory chemoreflex response in RTN neurons (Gestreau et al., 2010; Guyenet et al.,
285 2016; Kumar et al., 2015). As previously reported, the two pH sensors are expressed in the *Nmb*
286 cells of the RTN in partially overlapping populations of chemosensory neurons (Gestreau et al.,
287 2010; Kumar et al., 2015). In naïve rats 91.6 ± 11.2 % of *Nmb* cells were *Gpr4* positive, and 76.6 ±
288 14.8 % of *Nmb* cells were also *Task2* positive (n=4 rats). These values were not significantly
289 different in either NT-shRNA or PHOX2B shRNA rats (NT-shRNA: 90.0 ± 15.7% $Nmb^{+}/Gpr4^{+}$ and
290 76.2 ± 21.8% $Nmb^{+}/Gpr4^{+}$, n=10 rats; PHOX2B-shRNA: 89.4 ± 18.3% $Nmb^{+}/Gpr4^{+}$ and 75.6 ± 27.8%
291 $Nmb^{+}/Gpr4^{+}$, n=6 rats), suggesting that the fraction of *Nmb* cells expressing the two pH sensors
292 were not affected by the PHOX2B shRNA treatment.

293 Because it is not yet known whether PHOX2B controls the expression of GPR4 AND TASK2, we
294 quantified their single cell mRNA expression (CTCF) in *Nmb* cells of the RTN. Averaged cell
295 fluorescence for *Gpr4* and *Task2* mRNA in PHOX2B-shRNA rats was significantly reduced compared
296 to naïve and NT-shRNA rats (*Gpr4*: -34.4 ± 4.79% vs naïve, -27.9 ± 5.71% vs NT-shRNA $p<0.001$;
297 *Task2*: -39.0 ± 3.02% vs naïve, -34 ± 2.62% vs NT-shRNA $p<0.001$; Fig. 6B,D). To better understand
298 whether this reduction was ascribed to the specific loss of PHOX2B expression, we compared their
299 single cell mRNA expression levels between Nmb^{+}/PHOX2B^{-} and Nmb^{+}/PHOX2B^{+} neurons in
300 PHOX2B-shRNA rats. Both *Gpr4* and *Task2* mRNA expression was reduced in Nmb^{+}/PHOX2B^{-} cells
301 compared to Nmb^{+}/PHOX2B^{+} (*Gpr4*: -63.8 ± 3.9%; p= 0.022; *Task2*: -63.2 ± 2.77%; p= 0.029; Fig.
302 6C,E). Our data suggest that PHOX2B knockdown not only causes a reduction in the HCVR but also
303 a reduction in *Gpr4* and *Task2* mRNA levels in cells that are affected by PHOX2B knockdown.

304

305

306 **DISCUSSION**

307

308 The role of the transcription factor PHOX2B in the adult brain is still not fully understood. In this
309 study we reduced the expression of PHOX2B in the key chemosensory structure of the RTN with a
310 selective viral shRNA approach to test whether a knockdown of PHOX2B expression in these
311 neurons negatively impacts ventilation. Two weeks after viral infection we observed a modest
312 reduction of PHOX2B/*Nmb* expressing neurons in the RTN but no significant changes in basal V_E or
313 in the CO_2 chemoreflex. Four weeks after shRNA infection we observed a further reduction in the
314 expression of PHOX2B in *Nmb* neurons and a significant reduction of the CO_2 chemoreflex, while
315 ventilation in normoxia or hypoxia was unaffected. Furthermore, the level of expression of *Gpr4*
316 and *Task2* mRNAs, the two proton sensors responsible for the RTN neurons chemosensory
317 properties were significantly reduced in RTN neurons that lacked PHOX2B protein expression,
318 whereas *Nmb* mRNA expression level was unaffected by PHOX2B knockdown. These results
319 suggest that PHOX2B reduction affects the transcriptional activity of *Nmb* neurons in the RTN and
320 decreases the CO_2 response, possibly by reducing the expression of key proton sensors in the RTN.

321 **The role of PHOX2B in development and in the adult brain**

322

323 PHOX2B is a transcription factor with an important role in the development and differentiation of
324 neuronal structures in both the central and peripheral nervous system. Genetic loss of *Phox2b*
325 expression in mice shows that PHOX2B is essential for the correct development of all autonomic
326 ganglia in sympathetic, parasympathetic, and enteric nervous system and the distal ganglia of the
327 facial (VII), glossopharyngeal (IX), and vagus (X) cranial nerves (Pattyn et al., 1999), in addition to
328 carotid bodies and the solitary tract nucleus (Dauger, 2003). Furthermore, PHOX2B is involved in
329 the formation of all branchial and visceral hindbrain motor neurons and its absence during the
330 embryonic period impairs the development of motoneurons of the facial, trigeminal, ambiguus

331 and dorsal motor nucleus of the vagal nerve. PHOX2B is also necessary for the specification and
332 differentiation of the noradrenergic phenotype in multiple centres in the brain (Brunet & Pattyn,
333 2002; Pattyn et al., 1999, 2000a).
334 Interestingly, the expression of PHOX2B persists into adulthood in selected neuronal populations,
335 such as the ones involved in peripheral and central chemoreception, i.e., the carotid bodies, the
336 solitary tract nucleus and the RTN, in addition to neurons in the dorsal motor nucleus of the vagus,
337 the area postrema, the nucleus ambiguus, C1 catecholaminergic neurons and other scattered
338 neurons throughout the brainstem (Stornetta et al., 2006). Such widespread expression within the
339 adult brain suggests an important transcriptional role in neuronal survival and/or function. With
340 the exception of its role in maintaining the noradrenergic phenotype, its function in the postnatal
341 brain is unknown, in part because a full investigation of its transcriptional activity in neurons has
342 not yet been performed.
343 Heterozygote polyalanine expansion mutations in the exon 3 of *PHOX2B* are responsible for the
344 majority of cases of CCHS, a rare genetic disease that affect the autonomic nervous system and
345 central CO_2 chemoreflexes (Amiel et al., 2003; Di Lascio et al., 2021; Weese-Mayer et al., 2017).
346 While studies in transgenic mice expressing the mutated PHOX2B protein suggest that the RTN
347 may not form or be severely impaired (Dubreuil et al., 2008, 2009; Ramanantsoa et al., 2011), the
348 function of the wild-type protein in these neurons has never been tested beyond the post-natal
349 period. Thus, in order to determine whether PHOX2B is necessary for the survival and/or
350 chemosensory function of adult PHOX2B$^+$/*Nmb*$^+$ RTN neurons *in vivo*, we used a shRNA viral
351 approach to progressively knockdown the PHOX2B protein in these neurons.
352
353 **Modest reduction of PHOX2B in RTN does not impair ventilation**
354 Although the PHOX2B shRNA approach was not selective for *Nmb* neurons, we used small volumes
355 and localized injections to target the RTN. We identified RTN neurons by the mRNA expression of

356 the neuropeptide NMB (Shi et al., 2017) and observed a reduced number in both total *Nmb* and
357 *Nmb*$^+$/PHOX2B$^+$ neurons in PHOX2B shRNA treated rats compared to naïve and NT-shRNA rats two
358 weeks after viral infection. Interestingly, despite the small reduction in total *Nmb* cells of the RTN
359 in both NT-shRNA and PHOX2B-shRNA injected rats, possibly due to some off-target effects due to
360 activation of innate immunity or saturation of the microRNA pathway (Mcbride et al., 2008; Van
361 Gestel et al., 2014), no significant impairment in ventilation was observed. Even though PHOX2B
362 may be critical for chemosensory function in RTN neurons, the lack of significant ventilatory
363 impairment with a modest reduction of PHOX2B expressing neurons is not surprising. In our
364 previous study (and the ones of others), in which RTN chemosensory neurons were lesioned with
365 Substance P saporin toxin, CO_2-chemoreflex impairment became significant (~30% V_E Allo
366 reduction vs. pre-surgical baseline) only when *Nmb* neurons of the RTN (*Nmb*$^+$/PHOX2B$^+$ and
367 *Nmb*$^+$/PHOX2B$^-$ neurons) were reduced by ~63% compared to naïve controls (medium lesion
368 range: 50%-81% loss of *Nmb* neurons; Janes et al., 2024; Souza et al., 2023), therefore, even
369 though loss of PHOX2B severely altered the chemosensitive function in a fraction of *Nmb* cells, we
370 would not expect significant changes in ventilation only with a <50% RTN cell impairment or loss.
371

372 **Four weeks of PHOX2B knockdown impairs central CO_2 chemoreception**

373
374 Four weeks post- shRNA viral injection, the fraction of *Nmb*$^+$ cells expressing PHOX2B was further
375 reduced by 67% compared to naïve and by 61% compared to NT-shRNA rats. PHOX2B knockdown
376 was also restricted to RTN neurons, as adjacent C1 TH$^+$ neurons did not show any change in
377 number of TH$^+$/PHOX2B$^+$ expressing cells, although we can't exclude that some C1 cells may have
378 been infected, and their relative PHOX2B expression levels were slightly reduced. To support the
379 lack of significant alterations associated with the possible loss of C1 function was the lack of

380 significant changes in the hypoxic response that has been shown to be dependent on C1 neurons
381 (Malheiros-Lima et al., 2017).
382 Although we did not specifically quantify the relative mRNA expression change in intracellular
383 *Phox2b* levels within infected neurons, we measured the success of PHOX2B knockdown by
384 assessing the overall change in the number of *Nmb* cells that had no detectable levels of PHOX2B
385 protein in the nuclei. Thus, it is possible that this method led us to underestimate the success of
386 the overall PHOX2B shRNA knockdown in the RTN, as some RTN neurons may still have detectable
387 levels of PHOX2B, albeit decreased.
388 In PHOX2B-shRNA rats we did not observe any respiratory function changes in room air or in
389 hypoxia, similar to RTN lesioning studies (Janes et al., 2024; Souza et al., 2023; Guyenet et al.,
390 2019). When tested in hypercapnia though, PHOX2B-shRNA rats displayed a reduced HCVR
391 compared to both baseline (i.e., pre-surgery), naïve and NT-shRNA rats. The impairment of V_E Allo
392 was primarily a result of blunted V_T, and analysis of the convective exchange ratio (i.e. V_E/VO_2
393 ALLO) confirmed hypoventilation in 5% and 7.2% CO_2 only for PHOX2B-shRNA rats, suggesting a
394 specific impairment of chemosensitive properties in RTN neurons with PHOX2B knockdown.
395 These results are in line with previous studies in which medium RTN lesions (i.e. loss of >60 %
396 *Nmb*$^+$ cells) elicited by saporin toxin injection resulted in a significant CO_2-chemoreflex impairment
397 (Janes et al., 2024; Souza et al.,2018). Hence, killing RTN neurons or knocking down PHOX2B in
398 *Nmb* cells of the RTN gave comparable results.
399 Changes in the CO_2 response following 4 weeks of PHOX2B-shRNA treatment could occur because
400 the reduced expression of the transcription factor PHOX2B causes changes in the transcriptional
401 machinery of RTN neurons and alters transcription of CO_2/pH sensing proteins or other key
402 elements for their chemosensitive function. These transcriptional changes could also affect
403 neuronal survival. In fact, a small but significant loss of NMB expressing RTN neurons may

404 contribute to the reduction in the CO_2 response, although multiple studies have demonstrated
405 that significant cell loss must occur in the RTN in order to show a respiratory function impairment
406 (Janes et al., 2024; Souza et al.,2018; Nattie & Li, 2002; Takakura et al., 2008, 2014).
407 In our experiments, we observed a 35% reduction in total *Nmb*$^+$ cells compared to naïve rats and
408 23% compared to NT-shRNA, possibly due to cell death within the first 14 days post-infection.
409 Interestingly the loss of *Nmb* cells did not increase with time (although the fraction of
410 Nmb$^+$/PHOX2B$^+$ neurons decreased) and the central chemoreflex at 2 weeks post-surgery was not
411 impaired, suggesting that: i) the observed reduction in overall *Nmb* cell number in RTN occurring
412 in the first 2 weeks is not responsible for the CO_2 chemoreflex impairment that emerges 4 weeks
413 post-infection; ii) PHOX2B expression is most likely not necessary for neuronal survival of adult
414 *Nmb* neurons of the RTN; iii) a large reduction in *Nmb* neurons expressing PHOX2B$^+$ is necessary to
415 impair the HCVR (as we observed at 4 weeks). The interpretation that PHOX2B expression
416 contributes positively to the chemoreflex is further supported by our linear regression analysis
417 showing that *Nmb*$^+$/PHOX2B$^+$ cell number was the best predictor of the HCVR (r^2 = 0.739). The
418 initial cell loss, which we observed also in NT-shRNA, and more prominently with larger injection
419 volume of virus, may be attributed to some inherent cell death associated with the surgical
420 procedure (although not observed in similar studies performed by the same investigators, Janes et
421 al., 2024) or, more likely, with the potential off-target toxic effects associated with shRNA
422 procedures (Mcbride et al., 2008; Van Gestel et al., 2014).
423
424 **PHOX2B knockdown reduces mRNA expression of proton sensors in the Nmb cells of the RTN**
425 Current theories on central respiratory chemosensitivity postulate that changes in CO_2/pH in the
426 RTN are detected through two pH sensors, the proton-activated receptor GPR4 and the pH-
427 sensitive K^+ channel TASK2 that are expressed in partially overlapping populations of NMB
428 expressing RTN neurons (Kumar et al., 2015). Because it is not known whether PHOX2B has any

429 influence on the expression of TASK2, GPR4 or even the expression of the neuropeptide NMB used
430 to anatomically identify RTN neurons, we quantified their mRNA at cellular levels (calculated as
431 CFTC) and observed no changes in relative fluorescence of *Nmb* mRNA in the RTN relative to *Nmb*
432 levels in unrelated cells in the NTS, suggesting that *Nmb* expression is not affected by PHOX2B
433 shRNA knockdown and that *Nmb* is most likely not a target gene of PHOX2B in adult RTN neurons.
434 Furthermore, we determined the mRNA expression levels of *Task2* and *Gpr4* in both
435 *Nmb*$^+$/PHOX2B$^+$ and Nmb$^+$/PHOX2B$^-$ neurons in shRNA rats. Our results indicate that although the
436 fraction of *Nmb* cells of the RTN expressing *Gpr4* and *Task2* did not change across treatment, the
437 levels of *Gpr4* and *Task2* in *Nmb* neurons of PHOX2B-shRNA rats was reduced compared to the
438 naïve and NT-shRNA groups. Furthermore, there was a significant reduction of both *Gpr4* and
439 *Task2* levels within *Nmb*$^+$/PHOX2B$^-$ cells compared to *Nmb*$^+$/PHOX2B$^+$ cells. Because no good
440 antibodies are currently available to detect protein levels of either NMB, GPR4 or TASK2, our
441 results are only based on changes in mRNA levels, thus we can only speculate that a reduction in
442 *Gpr4* and *Task2* mRNA would translate in a reduction in the protein levels and consequent
443 reduction of RTN neurons chemosensitive properties. Direct electrophysiological recordings in RTN
444 neurons will be able to address the changes in CO_2/pH sensitivity of RTN neurons at cellular level.
445

446 **PHOX2B knockdown may impair CO_2-sensing through additional transcriptional targets**

447 Since loss of PHOX2B reduces expression of TH and dopamine beta hydroxylase enzymes in
448 catecholaminergic neurons *in vivo* and *in vitro* (Fan et al., 2011), it is possible that in NMB cells of
449 the RTN, reduction of PHOX2B alters the transcriptional machinery of other proteins (in addition
450 to GPR4 and TASK2) and impairs their function in central chemoreception. For example, a change
451 in the expression of enzymes, neurotransmitters, receptors, and ion channels in RTN neurons
452 could affect the excitatory signal transmission to preBötzinger Complex and the respiratory

453 network specifically during CO_2 challenges (Guyenet et al., 2016). Further studies will be needed to
454 address and identify additional transcriptional changes induced by PHOX2B knockdown *in vivo.*
455 An interesting observation from our histological data was the reduction in the overall number of
456 *Nmb* cells at two- and four-weeks following PHOX2B shRNA viral injections. Although some cell
457 death may be associated with either surgical procedures or off-target effects associated with the
458 shRNA approach (Mcbride et al., 2008; Van Gestel et al., 2014), it is intriguing to speculate that
459 loss of PHOX2B expression may have some effects on viability of RTN neurons *in vivo*. Even though
460 this is a possibility, especially with an even more severe knockdown, we did observe a large
461 proportion of *Nmb* cells devoid of PHOX2B protein expression, suggesting that absence of PHOX2B
462 is compatible with neuronal survival, at least in our experimental time frame.
463
464 **Relevance to CCHS and its pathogenic mechanisms**
465 Our results contribute to further our understanding on potential pathogenic mechanisms in CCHS
466 (Di Lascio et al., 2018). Homozygous knockout mice for PHOX2B die during gestation (Pattyn et al.,
467 1999, 2000) demonstrating a key role of this transcription factor in cellular proliferation, migration
468 and differentiation during embryonic development, whereas heterozygotes for PHOX2B survive
469 birth and live into adulthood, but display apneas (Durand et al., 2005) and impairment of the
470 hypoxic and hypercapnic ventilatory responses in the neonatal period (Dauger, 2003). Here we
471 show that, independent of the PHOX2B role during development, PHOX2B is still required to
472 maintain proper CO_2 chemoreflex responses in the adult brain.
473 Heterologous expression of the mutant PHOX2B alters development of RTN in mice and impairs
474 their chemoreflex response (Dubreuil et al., 2008, 2009). The effects of the expression of the
475 mutant PHOX2B on wild-type PHOX2B protein and its transcriptional activity is not known *in vivo*
476 yet, although *in vitro* data indicates that the mutated PHOX2B protein alters wild-type PHOX2B
477 conformation and its ability to form homo- and hetero-dimers (Di Lascio et al., 2016; Trochet et

478 al., 2005, 2008), its affinity for DNA and coactivators, as well as its degradation rate (Nagashimada
479 et al., 2012; Wu et al., 2009). It has also been shown that mutant PHOX2B causes the formation of
480 cytoplasmic aggregates (Bachetti et al., 2005; Trochet et al., 2005, 2008) and fibrils *in vitro* (Pirone
481 et al., 2019), and dysregulates the transcriptional function of wild-type PHOX2B (Di Lascio et al.,
482 2013; Parodi et al., 2012), thus changing expression of important target genes such as DBH,
483 PHOX2A and TLX2 (Bachetti et al., 2005; Di Lascio et al., 2013; Trochet et al., 2005). Based on this
484 evidence, different CCHS pathogenic mechanisms have been proposed (e.g., PHOX2B loss-of-
485 function, dominant-negative or toxic function of the mutant protein) including gene and cell
486 specific transcriptional dysregulation (Di Lascio et al., 2018, 2021). Interestingly, only a handful of
487 PHOX2B target genes have been identified and the function of PHOX2B and its mutated forms in
488 respiratory control and CCHS pathogenesis is still under investigation.
489 Our data suggest that, in addition to potential effect of mutated PHOX2B on development and
490 cellular function in CCHS pathogenesis, the expression of wild type PHOX2B has an important role
491 in respiratory control that extends the developmental period and its reduction in CCHS may
492 contribute to the respiratory impairment in this disorder.

493

494 **MATERIALS AND METHODS**

495 Experiments were performed using male Sprague–Dawley rats (starting weight range 250-350g)
496 born in the University of Alberta animal facility to pregnant dams obtained from Charles River
497 (Senneville, QC). Rats were housed at the University of Alberta Health Sciences Animal Housing
498 Facility and maintained on a 12-hr dark/light cycle with food and water available *ad libitum*.
499 Handling and experimental procedures were approved by the Health Science Animal Policy and
500 Welfare Committee at the University of Alberta (AUP#461) and performed in accordance with
501 guidelines established by the Canadian Council on Animal Care.

502

503 **ShRNA viral injection in the retrotrapezoid nucleus**

504 In order to knockdown Phox2b expression at the level of RTN neurons, we used a mix of two
505 shRNA clones targeting two different sequences of the Phox2b mRNA carried by a non-replicating
506 lentivirus vector ($1x10^9$ VP/ml; TRCN000041283: GCCTTAGTGAAGAGCAGTATG and
507 TRCN0000096437: CCTCTGCCTACGAGTCCTGTA; Sigma Aldrich, St. Louis, MA, USA). The shRNAs
508 were designed against the Phox2b mouse sequence (Ref Seq NM_008888) which shares 100%
509 homology with the Phox2b rat sequence (Ref Seq XM_008770167).

510 Metacam analgesic was administered 1 hour prior to surgery (2mg/kg) to reduce post-surgical
511 pain. Rats were anesthetized with a ketamine/xylazine mixture (100mg/kg + 10mg/kg,
512 respectively; i.p.); the anaesthetic level was assessed by lack of paw pinch reflex and maintenance
513 of a regular breathing rate. Additional anaesthesia was administered as needed. The rat was
514 positioned on a stereotactic apparatus (Kopf Instruments, Tujunga, CA, USA) and a total of four
515 microinjections (200 or 100 nL per injection; two rostro-caudally aligned injections per side) were
516 made lateral to the midline and ventral to the facial motor nucleus under aseptic conditions.
517 Coordinates were as follows in mm from obex (medio-lateral/rostro-caudal/dorso-ventral): ±1.8,
518 +2.0,-3.5; ±1.8,+2.4,-3.6. Injections were made using a glass microelectrode (30 µm diameter tip,
519 Drummond Scientific, PA, USA). Twenty-five rats (8 rats 200nl/injection; 17 rats 100nl/injection)
520 underwent shRNA viral injection (PHOX2B-shRNA) and 23 rats (6 rats 200nl/injection; 17 rats
521 100nl/injection) received a non-target shRNA viral injection (NT-shRNA; SHC016:
522 MISSION® pLKO.1-puro non-Target shRNA Control Plasmid DNA; Sigma Aldrich, St. Louis, MA, USA)
523 to determine any effects of surgery and viral constructs on respiratory behaviour. Eight naïve rats,
524 receiving no surgery and maintained in the same housing conditions, were used as additional
525 controls for both respiratory function and anatomical experiments. Following each injection, the

526 glass electrodes were left in place for 3-5 minutes to minimize backflow of virus up the electrode
527 track. At the end of the surgery, the incision was sutured, and rats received local anaesthetic
528 bupivacaine (0.1 mL, s.c.) and were treated with metacam analgesic for 72 hours. Rats recovered
529 for 7 days before the next respiratory function testing.

530

531 **Data acquisition and analysis of respiratory measurements**

532 Rats were habituated to whole-body plethysmography chambers (Buxco, 5L) once, 3-4 days before
533 baseline recordings. On the day of the experiment, rats were placed in the chamber and testing
534 commenced once the animals were quietly awake (typically 20-30 mins). Gas mixtures were
535 delivered at 1.5 L/min using a GSM-3 (CWE Inc., Ardmore, PA, USA) and monitored using a Gas
536 Analyzer (AD Instruments, Sydney, Australia). Ventilatory parameters were measured during
537 exposure to different air compositions for 8-15 min each. Room air: 21%O_2 + 0%CO_2 (balanced
538 with N_2); Normoxic Hypercapnia: 21%O_2+ 5%CO_2; 21%O_2 + 7.2%CO_2; Normocapnic Hypoxia:
539 10.6%O_2+ 0% CO_2.

540 As previously described (Cardani et al., 2022; Janes et al., 2024) respiratory data were analysed
541 from rats during quiet wakefulness in the last 5 min period of each gas composition using the
542 barometric method (open-flow system; Cardani et al., 2022; Janes et al., 2024; Mortola & Frappell,
543 1998; Seifert et al., 2000). Raw pressure signals were acquired with a Validyne differential
544 pressure transducer connected to a CD15 carrier demodulator (Validyne Engineering, Northridge,
545 CA, USA) and digitized using a Powerlab 8/35 (AD Instruments, Sydney, Australia). Analysis was
546 done using Labchart 8 (v8.1.19, AD Instruments, Colorado Springs, CO, USA) to determine tidal
547 volume (V_T) and breathing frequency (f_R). The amplitude of the pressure signal was converted to
548 V_T (ml·kg^{-1}) using the equations of Drorbaug and Fenn 1955 (Drorbaugh & Fenn, 1955) and

549 calibrated against 1 mL of dry air injected into the empty chamber using a rodent ventilator
550 (Harvard Rodent Ventilator Model 683, Holliston, MA, USA ƒ = 50, 75, 100, 150 beats·min^{-1}).
551 Humidity and chamber temperature were monitored using a RH-300 water vapour analyzer (Sable
552 Systems, Las Vegas, NV, USA) and a HPR Plus Handheld PIT Tag reader (Biomark, Boise, ID, USA)
553 respectively, depending on the setup. Rectal temperature was read through the temperature
554 probes of a Homeothermic Monitor (507222F, Harvard Apparatus, Holliston, MA, USA). Minute
555 ventilation ($\dot{V}_E$) was calculated as f_R x V_T and expressed as ml·min^{-1}·kg^{-1}. Rats gained, on average,
556 160 ± 4g over the experimental paradigm (naive: 158 ± 19g; NT-shRNA: 202 ± 25g; PHOX2B-shRNA:
557 133 ± 7g); we therefore applied an allometric correction to $\dot{V}_E$ to account for non-linear effects of
558 weight gain (V_E ALLO) (Mortola et al., 1994).

559 Metabolic parameters VO_2 and V_E/VO_2 were calculated by pull-mode indirect calorimetry and
560 allometrically scaled to be consistent with ventilation (Mortola et al., 1994). The % composition of
561 dry gas flowing into, and out of the recording chamber was measured by using an AD Instruments
562 Gas Analyzer (Colorado Springs, CO) and applying the equations of Depocas and Hart (Depocas F,
563 Hart JS, 1957) and Lighton (Lighton, 2021).

564 Weight measurements were taken prior to every recording session. Rats breathing function was
565 measured the week prior to surgery (baseline recording) and weekly following shRNA injections to
566 determine the time course of ventilatory impairment.

567 Respiratory data were compared for naive, NT-shRNA and PHOX2B-shRNA pre- and post-injection
568 using a mixed factor ANOVA (independent factor = treatment, repeated measures factor = pre-
569 and post-lesion; Fig.1,4). Post-hoc analysis used the Bonferroni correction factor, with $p<0.05$
570 considered to be significant. Ventilatory data are reported as mean ± standard deviation (SD).

571

572 **In Situ hybridization (RNAScope) and immunofluorescence**

573 Either 2 or 4-weeks after viral injection, rats were transcardially perfused with saline 0.9% NaCl
574 followed by 4% paraformaldehyde (PFA) and the brains were post-fixed in 4% PFA overnight and
575 cryoprotected in 30% sucrose in 1X Phosphate Buffered Saline (PBS). Brains were then frozen in
576 O.C.T compound (Fisher Scientific) and sectioned on a cryostat (MODEL CM1950, Leica
577 Biosystems, Buffalo grove, IL, USA) at 30 µm and stored in cryoprotectant buffer at -20°C until
578 processing. Sections were mounted on slides for combined RNAScope® in situ hybridization
579 (Advanced Cell Diagnostics-ACD Bio, Newark CA, USA) and immunofluorescence assay and
580 processed as previously detailed (Biancardi et al., 2021; Cardani et al., 2022). The mRNA
581 expression for *Neuromedin B* (*Nmb)* was used as marker of RTN CO_2-sensing neurons (Shi et al.,
582 2017). Slides were incubated with probes for *Nmb* (Rn-NMB-C2 #494791-C2, ACDBio, Newark, CA,
583 USA), *Phox2b* (Rn-Phox2b-O1-C1 #1064121-C1, ACDBio), G-protein-coupled receptor 4 (*Gpr4*)
584 (Mm-Gpr4-C1, #427941, ACDBio), and potassium channel, subfamily K, member 5 (*Kcnk5* or *Task-*
585 *2*) (Mm-Kcnk5-C3, #427951-C3, ACDBio) for 2 hr at 40°C. Gpr4 and Kcnk5 probes are design against
586 the mouse mRNA sequence (Ref Seq NM_175668.4 and NM_021542.4, respectively). However,
587 the alignment of the mouse mRNA sequences with those of rat (GPR4: Ref Seq NM_001025680.1;
588 TASK2: Ref Seq NM_1039516.2) showed an identity of 94% and 96%, respectively, at the level of
589 the target region (Base Pairs 1030-150) (BLAST® program, National Library of Medicine, National
590 Center for Biotechnology Information, NIH). In parallel, two sections/rat were treated with
591 positive (low copy housekeeping gene), and negative (non-specific bacterial gene) control probes
592 provided by ACDBio. Finally, slides were processed using the RNAScope Multiplex Fluorescent
593 Assay kit V2 (ACDBio) according to the manufacturer's instructions. The probes were visualized
594 using Opal 520 and Opal 570 reagent (1:500 and 1:1000, respectively; PerkinElmer, Woodbridge,
595 ON, CA). PHOX2B immunoreactivity was detected using mouse monoclonal PHOX2B antibody (B-

596 11: sc-376997, 1:100, Santa Cruz Biotechnology) incubated overnight in 0.3% TritonX-100, 1%NDS
597 in PBS followed by donkey CY5-conjugated anti-mouse IgG (1:200; Jackson Immuno Research
598 Laboratories Inc) in PBS + 1% NDS for 2 hours. Slides were then washed in PBS and cover-slipped
599 with Fluorosave mounting media (EMD Millipore).

600 We also performed staining for tyrosine hydroxylase (TH) to identify and quantify C1 cells
601 (TH^+/$PHOX2B^+$) following shRNA injection. Briefly, perfusion and tissue fixation/freezing were done
602 as described above. Floating sections were stained with rabbit anti TH antibody (AB152,1:1000,
603 Millipore SIGMA, USA), and mouse anti PHOX2B (B-11: sc-376997, 1:100, Santa Cruz
604 Biotechnology). Antibodies were visualized using donkey CY3 (TH) and CY5 (PHOX2B) conjugated
605 IgG (1:200; Jackson Immuno Research Laboratories Inc). The sections were washed in PBS and
606 mounted on slides and cover-slipped with Fluorosave mounting media.

607

608 **Cell counting, imaging and data analysis.**

609 To quantify *Nmb*+/PHOX2B- and *Nmb*+/PHOX2B+ neurons within the RTN region, we analysed one
610 every seven sections (210 µm interval; 8 sections/rat in total) along the rostrocaudal distribution
611 of the RTN on the ventral surface of the brainstem and compared total bilateral cell counts of
612 PHOX2B-shRNA rats with non-target control (NT-shRNA) and naïve rats. Cells that expressed *Nmb*
613 and *Phox2b* mRNAs but did not show co-localization with PHOX2B protein were considered
614 *Nmb*+/PHOX2B-.

615 The Corrected Total Cell Fluorescence (CTCF) signal for *Nmb, Gpr4* and *Task2* mRNAs was
616 quantified as previously described (Cardani et al., 2022; McCloy et al., 2014). Briefly, a Leica TCS
617 SP5 (B-120G) Laser Scanning Confocal microscope was used to acquire images of the tissue.
618 Exposure time and acquisition parameters were set for the naïve group and kept unchanged for

619 the entire dataset acquisition. The collected images were then analysed by selecting a single cell at
620 a time and measuring the area, integrated density and mean grey value (McCloy et al., 2014). For
621 each image, three background areas were used to normalize against autofluorescence. We used 4
622 sections/rat (210 µm interval) to count *Nmb*, *Gpr4* and *Task2* mRNA CTCF in the core of the RTN
623 area where several *Nmb* cells could be identified. For each section, two images were acquired with
624 a 20× objective, so that at least fifty cells per tissue sample were obtained for the mRNA
625 quantification analysis. To evaluate changes in *Nmb* mRNA expression levels following PHOX2B
626 knockdown at the level of the RTN, we compared, the fluorescence intensity of each RTN *Nmb* cell
627 (223.2 ± 37.1 cells/animal) with the average fluorescent signal of *Nmb* cells located dorsally in the
628 NTS (4.3 ± 1.2 cells/animal) (*Nmb* CTCF ratio RTN/NTS) as we reasoned that the latter would not
629 be affected by the shRNA infection and knockdown.

630 To quantify *Gpr4* and *Task2* mRNA expression in *Nmb* cells of the RTN, we first quantified single
631 cell CTCF for either *Gpr4* (200.7 ± 13.2 cells/rat) or *Task2* (169.6 ± 10.3 cells/rat) mRNA in *Nmb*
632 cells of the RTN in the 3 experimental groups (naïve, NT shRNA and PHOX2B shRNA) independent
633 of their PHOX2B expression. We then compared CTCF values of *Gpr4* and *Task2* mRNA between
634 Nmb^{+}/PHOX2B^{+} and Nmb^{+}/PHOX2B^{-} RTN neurons in PHOX2B-shRNA rats to address changes in
635 their mRNA expression induced by PHOX2B knockdown.

636 To assess whether shRNA knockdown affected either the number or the expression of PHOX2B in
637 TH expressing C1 neurons, we counted the number of TH^{+}/PHOX2B^{+} and TH^{+}/PHOX2B^{-} cells along
638 the ventrolateral medulla (8 sections/rat; 240 µm interval) using an EVOS fluorescent microscope
639 (ThermoFisher Scientific).

640 Digital colour photomicrographs were acquired using a Leica TCS SP5 (B-120G) Laser Scanning
641 Confocal microscope. Image J (version 1.54f; National Institutes of Health, Bethesda, MD, USA)
642 and Excel (Microsoft Office 365 for Windows) were used for cell counting and the measurements

643 of fluorescence intensity. Statistical analysis of cell counts, and fluorescent signals was made using
644 one- way ANOVA (Fig. 2C, 3C, S1B) and repeated-measures ANOVA (Fig 5B, D and 6) with
645 GraphPad Prism 8 Software (GraphPad Software, Inc., San Diego, CA, USA). Linear regressions to
646 determine the effect of cell counts (*Nmb*$^{+}$/PHOX2B^{+}, *Nmb*$^{+}$/PHOX2B^{-}, total cells) on chemoreflex
647 magnitude were run using a combined dataset for naive, NT-shRNA and PHOX2B-shRNA rats (SPSS
648 version 13.0; Fig.5E-F). p values of < 0.05 were considered significant and data are reported as
649 mean ± standard deviation (SD).

650

651

652

653 **FIGURE LEGENDS**

654 **Figure 1. Respiratory data two weeks post viral PHOX2B shRNA injection**. **(A)** breathing
655 frequency (f_R,), **(B)** tidal volume (V_T), **(C)** allometric minute ventilation (V_E ALLO), **(D)** oxygen
656 consumption (VO_2 ALLO), **(E)** convective requirement ratio (V_E/VO_2 ALLO), **(F)** hypercapnic
657 ventilatory response (HCVR absolute change in V_E ALLO vs. corresponding room air) of baseline
658 (pre-surgery, grey filled box), naïve (black n=8), non-target control shRNA (NT-shRNA, grey n=17)
659 and PHOX2B shRNA (PHOX2B-shRNA, red n=17) rats 2-weeks post injection during room air,
660 hypercapnia 5% and 7.2% CO_2. f_R is equally impaired in all experimental group compared to
661 baseline but no treatment effect was observed (A). V_T is significantly impaired following RTN
662 injection in PHOX2B-shRNA group compared to naïve animals ($p=0.022$) and baseline ($p< 0.001$) at
663 7.2% CO_2 (B). V_E ALLO is increased in naïve rats compared to the other treatment groups ($p=0.005$)
664 in room air (C). Boxplots: median, 1st – 3rd quartiles and 10th – 90th percentiles, outliers = dots, "+"
665 indicates arithmetic mean. Bonferroni post-hoc as indicated. Black*, different from naïve; Grey*,
666 different from NT-shRNA; Red*, different from PHOX2B- shRNA.

667

668

669 **Figure 2. PHOX2B and *Nmb* expression and total cell count within the RTN area in naïve, NT-**
670 **shRNA and PHOX2B-shRNA injected rats two weeks post viral shRNA injection. (A)** Schematic
671 and representative image of a transverse brainstem section at the level of the RTN (-11.5 mm
672 distance from Bregma) showing the area of investigation containing RTN neurons. **(B)** Expression
673 of *Phox2b* mRNA (red), PHOX2B protein (white) and *Nmb* mRNA (green) in RTN Nmb^+/PHOX2B$^+$
674 and Nmb^+/PHOX2B$^-$ neurons in naïve (left), NT-shRNA (middle), and PHOX2B-shRNA (right) rats
675 (magnified view inserts below). Arrowheads indicate absence of PHOX2B protein. Scale

676 bar=400µm (top figures), 150µm (inserts below). **(C)** The number of total cells (*Nmb*$^{+}$/PHOX2B^{+}
677 plus *Nmb*$^{+}$/PHOX2B^{-}) comprising the RTN are reduced in PHOX2B-shRNA rats (n=4) as compared to
678 naïve (n=4) and NT-shRNA (n=4), and in NT-shRNA rats as compared to naïve rats (black$^{\#}$, One-way
679 ANOVA, p<0.001). The number of *Nmb*$^{+}$/PHOX2B^{+} cells are reduced in PHOX2B-shRNA rats as
680 compared to naïve and NT-shRNA (Blue*, One-way ANOVA, p<0 0.001). The number of
681 *Nmb*$^{+}$/PHOX2B^{-} cells was unchanged across groups. **(D,E)** Rostral-caudal distribution (distance
682 from the caudal tip of the facial nucleus, 7Mn) of *Nmb*$^{+}$/PHOX2B^{+} (D) and *Nmb*$^{+}$/PHOX2B^{-} (E)
683 neurons along the RTN.

684

685 **Figure 3. PHOX2B and *Nmb* expression and total cell count within the RTN area in naïve, NT-**
686 **shRNA and PHOX2B-shRNA injected rats 4 weeks post viral shRNA injection. (A)** Schematic and
687 representative image of a transverse brainstem section at the level of the RTN (-11.5 mm distance
688 from Bregma) showing the area of investigation containing RTN neurons. **(B)** Expression of *Phox2b*
689 mRNA (red), PHOX2B protein (white) and *Nmb* mRNA (green) in naïve (left), NT-shRNA (middle),
690 and PHOX2B-shRNA (right) rats (magnified view insert). Arrowheads indicate absence of PHOX2B
691 protein. Scale bar = 400µm (top figures), 150µm (inserts below). **(C)** The number of total cells
692 (*Nmb*$^{+}$/PHOX2B^{+} + *Nmb*$^{+}$/PHOX2B^{-}) comprising the RTN are reduced in PHOX2B-shRNA rats (n=6)
693 as compared to naïve (n=4) (Black$^{\#}$, One-way ANOVA, p=0.0087) but not to NT-shRNA (n=10). The
694 number of *Nmb*$^{+}$/PHOX2B^{+} cells are reduced in PHOX2B-shRNA rats as compared to naïve and NT-
695 shRNA (Blue*, one-way ANOVA, p<0.001). The number of *Nmb*$^{+}$/PHOX2B^{-} cells are increased in
696 PHOX2B-shRNA rats as compared to both naïve and NT-shRNA (Green*, one-way ANOVA
697 p<0.001). **(D, E)** Rostral-caudal distribution (distance from the caudal tip of the facial nucleus,
698 7Mn) of *Nmb*$^{+}$/PHOX2B^{+} (D) and *Nmb*$^{+}$/PHOX2B^{-} (E) neurons along the RTN.

699

700 **Figure 4. Respiratory data following 4 weeks post viral shRNA injection**. **(A)** breathing frequency
701 (f_R,), **(B)** tidal volume (V_T), **(C)** allometric minute ventilation (V_E ALLO), **(D)** convective requirement
702 ratio (V_E/VO_2 ALLO), **(E)** hypercapnic ventilatory response (HCVR, absolute change in V_E ALLO vs.
703 corresponding room air), **(F)** HCVR at baseline, week 2 and week 4 post-viral injections in naïve
704 (black n=8), non-target control shRNA (NT-shRNA, grey n=10) and PHOX2B-shRNA (PHOX2B-
705 shRNA, red n=6). f_R is equally impaired in all experimental group compared to baseline but no
706 treatment effect was observed (A). V_T is significantly impaired following RTN injection in PHOX2B-
707 shRNA group compared to baseline pre-surgery (p<0.001), naïve rats p<0.001), and NT-shRNA rats
708 (p=0.002) at 7.2% CO_2. (B). V_E ALLO is impaired in PHOX2B-shRNA rats during exposure to
709 hypercapnia (7.2% CO_2) compared to baseline (p=0.0025), naïve rats (p=0.007), and NT-shRNA rats
710 (p=0.002). (C). V_E/VO_2 ALLO is reduced in PHOX2B-shRNA animals compared to NT-shRNA rats
711 both at 5% (p=0.023) and 7.2% (p=0.004.) CO_2 (D). HCVR during 7.2% CO_2 is lower in PHOX2B-
712 shRNA rats compared to baseline (p=0.007), naïve rats (p=0.001), and NT-shRNA rats (p=0.016) (E).
713 Boxplots: median, 1st – 3rd quartiles and 10th – 90th percentiles, outliers = dots, "+" indicates
714 arithmetic mean. Bonferroni post-hoc as indicated. HCVR is significantly impaired only in PHOX2B-
715 shRNA rats 4-weeks post-surgery (One-way ANOVA p=0.007) (F). Black*, different from naïve;
716 Grey*, different from NT-shRNA; Red*, different from PHOX2B- shRNA.

717

718 **Figure 5. PHOX2B knockdown in RTN neurons does not alter TH or *Nmb* expression but impairs**
719 **the hypercapnic ventilatory response. (A)** PHOX2B protein (white) and TH (red) expression in C1
720 neurons of naïve (left), NT-shRNA (middle), and PHOX2B-shRNA (right) rats. Magnified view at the
721 bottom. Arrowheads indicate the colocalization of PHOX2B and TH protein in C1 neurones cells.
722 Scale bar = 400µm (top figures), 150µm (bottom figures). **(B)** No differences are observed in the
723 rostral-caudal distribution of $TH^+/PHOX2B^+$ catecholaminergic C1 neurons cells caudal to the RTN

724 between naïve (black, n=4), NT-shRNA (grey, n=10) and PHOX2B-shRNA (red, n=6) rats. **(C)**
725 PHOX2B protein (white) and *Nmb* mRNA (green) expression in NT-shRNA rat at the level of NTS
726 and RTN regions. Magnified view on the left. Arrowheads indicate cells with *Nmb* mRNA
727 expression. Scale bar = 400µm (right figures), 150µm (left figures). **(D)** Quantification of single
728 cells *Nmb* mRNA fluorescence intensity along the rostro-caudal extension of RTN in naïve (black,
729 n=4), NT-shRNA (grey, n=10) and PHOX2B-shRNA (red, n=6) rat calculated as average ratio
730 between RTN and NTS cells shows no difference between treatment groups. Data are shown as
731 average cell fluorescence value at different rostro-caudal levels. **(D-E)** X-Y plot of HCVR during
732 7.2% CO_2 exposure relative to the number of *Nmb*$^+$/PHOX2B$^+$ (D, slope is different from "0" at
733 $p<0.001$; $r^2=0.739$) and *Nmb*$^+$/PHOX2B$^-$ (E, $p<0.001$ for difference between slopes; $r^2=0.482$) in the
734 RTN.

735

736 **Figure 6. *Gpr4* and *Task2* mRNA expression within the RTN area in naïve, and PHOX2B-shRNA**
737 **injected rats 4 weeks post viral shRNA injection. (A,D)** *Nmb* (green), *Gpr4*, *Task2* mRNA (red) and
738 PHOX2B protein (grey) expression in RTN neurons in naïve (top) and PHOX2B-shRNA (bottom) rats.
739 Scale bar = 150 µm. Arrowheads indicate colocalization of *Gpr4* (A) and *Task2* (D) with
740 *Nmb*$^+$/PHOX2B$^+$ neurons. Asterisks indicate colocalization of *Gpr4* (A) and *Task2* (D) with
741 *Nmb*$^+$/PHOX2B$^-$ neurons. **(B,E)** Quantification of single cells *Gpr4* and *Task2* mRNA fluorescence
742 intensity along the rostro-caudal extension of RTN in naïve (black), NT-shRNA (grey) and PHOX2B-
743 shRNA (red) rats. Black*, different from naïve, Grey*, different from NT-shRNA (**C and F**)
744 Quantification of single cells *Gpr4* and *Task2* mRNA fluorescence staining intensity along the
745 rostro-caudal extension of RTN in Nmb$^+$/PHOX2B$^+$ (red filled dot) and Nmb$^+$/PHOX2B$^-$ (red empty
746 dot) neurons in PHOX2B-shRNA rats. Data are shown as average cell fluorescence value at
747 different rostro-caudal levels of the RTN. Mean corrected total cell fluorescence (CTCF) value ±

748 SEM combined (naïve, n=4; NT-shRNA, n=10; PHOX2B-shRNA, n=6) (see methods for detail). One-
749 way ANOVA repeated measures.

750

751 **Supplementary Fig. 1. (A)** Allometric V_E is equally impaired following RTN injection of non-target
752 control (NT-shRNA n=6) and PHOX2B-shRNA (n=8). Asterisks, difference from baseline. **(B)** The
753 number of Nmb^+/$PHOX2B^+$ cells comprising the RTN are reduced in NT-shRNA (n=5), and shRNA
754 rats (n=5) as compared to naive controls (n=4; Asterisks, difference from baseline). The number of
755 Nmb^+/$PHOX2B^-$ cells was unchanged in both surgical treatments compared to baseline.

756
757 **Supplementary table 1.** Summary of statistical tests and results presented in the figures.

758 **REFERENCES**

759 Abbott, S. B. G., Stornetta, R. L., Coates, M. B., & Guyenet, P. G. (2011). *Phox2b-Expressing*
760 *Neurons of the Parafacial Region Regulate Breathing Rate, Inspiration, and Expiration in*
761 *Conscious Rats*. https://doi.org/10.1523/JNEUROSCI.3280-11.2011

762 Amiel, J., Laudier, B., Attié-Bitach, T., Trang, H., De Pontual, L., Gener, B., Trochet, D., Etchevers, H.,
763 Ray, P., Simonneau, M., Vekemans, M., Munnich, A., Gaultier, C., & Lyonnet, S. (2003).
764 Polyalanine expansion and frameshift mutations of the paired-like homeobox gene PHOX2B in
765 congenital central hypoventilation syndrome. *Nature Genetics*, *33*(4), 459–461.
766 https://doi.org/10.1038/ng1130

767 Bachetti, T., Matera, I., Borghini, S., Duca, M. Di, Ravazzolo, R., & Ceccherini, I. (2005). Distinct
768 pathogenetic mechanisms for PHOX2B associated polyalanine expansions and frameshift
769 mutations in congenital central hypoventilation syndrome. *Human Molecular Genetics*, *14*(13),
770 1815–1824. https://doi.org/10.1093/hmg/ddi188

771 Barna, B. F., Takakura, A. C., Mulkey, D. K., & Moreira, T. S. (2016). Purinergic receptor blockade in
772 the retrotrapezoid nucleus attenuates the respiratory chemoreflexes in awake rats. *Acta*
773 *Physiologica (Oxford, England)*, *217*(1), 80–93. https://doi.org/10.1111/APHA.12637

774 Basting, T. M., Burke, P. G. R., Kanbar, R., Viar, K. E., Stornetta, D. S., Stornetta, R. L., & Guyenet, P.
775 G. (2015). *Hypoxia Silences Retrotrapezoid Nucleus Respiratory Chemoreceptors via Alkalosis*.
776 https://doi.org/10.1523/JNEUROSCI.2923-14.2015

777 Berry-Kravis, E. M., Zhou, L., Rand, C. M., & Weese-Mayer, D. E. (2006). Congenital central
778 hypoventilation syndrome PHOX2B mutations and phenotype. *American Journal of Respiratory*
779 *and Critical Care Medicine*, *174*(10), 1139–1144. https://doi.org/10.1164/rccm.200602-305OC

780 Biancardi, V., Saini, J., Pageni, A., Prashaad M., H., Funk, G. D., & Pagliardini, S. (2021). Mapping of
781 the excitatory, inhibitory, and modulatory afferent projections to the anatomically defined
782 active expiratory oscillator in adult male rats. *Journal of Comparative Neurology*, *529*(4), 853–
783 884. https://doi.org/10.1002/CNE.24984

784 Bourdeaut, F., Trochet, D., Janoueix-Lerosey, I., Ribeiro, A., Deville, A., Coz, C., Michiels, J. F.,
785 Lyonnet, S., Amiel, J., & Delattre, O. (2005). Germline mutations of the paired-like homeobox 2B
786 (PHOX2B) gene in neuroblastoma. In *Cancer Letters* (Vol. 228, Issues 1–2, pp. 51–58). Elsevier.
787 https://doi.org/10.1016/j.canlet.2005.01.055

788 Brunet, J. F., & Pattyn, A. (2002). Phox2 genes - From patterning to connectivity. In *Current Opinion*
789 *in Genetics and Development* (Vol. 12, Issue 4, pp. 435–440). https://doi.org/10.1016/S0959-
790 437X(02)00322-2

791 Cardani, S., Janes, T. A., Saini, J. K., Di Lascio, S., Benfante, R., Fornasari, D., & Pagliardini, S. (2022).
792 Etonogestrel Administration Reduces the Expression of PHOX2B and Its Target Genes in the
793 Solitary Tract Nucleus. *International Journal of Molecular Sciences*, *23*(9).
794 https://doi.org/10.3390/ijms23094816

795 Cutsforth-Gregory, J. K., & Benarroch, E. E. (2017). Nucleus of the solitary tract, medullary reflexes,
796 and clinical implications. *Neurology*, *88*(12), 1187–1196.
797 https://doi.org/10.1212/WNL.0000000000003751

798 Dauger, S. (2003). Phox2b controls the development of peripheral chemoreceptors and afferent
799 visceral pathways. *Development*, *130*(26), 6635–6642. https://doi.org/10.1242/dev.00866

800 Depocas, F., & Sanford Hart, J. (n.d.). *Use of the Pdzlling Oxygen Analyzer for Memwement of*
801 *Oxygen conszlm~tion of Ahmds iti Open-Circuit Systems ad in a Short-Lag, Closed-Cirwit Appma*
802 *tml*.

803 Di Lascio, S., Bachetti, T., Saba, E., Ceccherini, I., Benfante, R., & Fornasari, D. (2013).
804 Transcriptional dysregulation and impairment of PHOX2B auto-regulatory mechanism induced
805 by polyalanine expansion mutations associated with congenital central hypoventilation
806 syndrome. *Neurobiology of Disease*, *50*(1), 187–200. https://doi.org/10.1016/j.nbd.2012.10.019

807 Di Lascio, S., Belperio, D., Benfante, R., & Fornasari, D. (2016). Alanine expansions associated with
808 congenital central hypoventilation syndrome impair PHOX2B homeodomain-mediated
809 dimerization and nuclear import. *Journal of Biological Chemistry*, *291*(25), 13375–13393.
810 https://doi.org/10.1074/jbc.M115.679027

811 Di Lascio, S., Benfante, R., Cardani, S., & Fornasari, D. (2018). Advances in the molecular biology
812 and pathogenesis of congenital central hypoventilation syndrome—implications for new
813 therapeutic targets. *Expert Opinion on Orphan Drugs*, *00*(00), 1–13.
814 https://doi.org/10.1080/21678707.2018.1540978

815 Di Lascio, S., Benfante, R., Cardani, S., & Fornasari, D. (2021). Research Advances on Therapeutic
816 Approaches to Congenital Central Hypoventilation Syndrome (CCHS). *Frontiers in Neuroscience*,
817 *14*. https://doi.org/10.3389/FNINS.2020.615666

818 Di Lascio, S., Benfante, R., Zanni, E. Di, Cardani, S., Adamo, A., Fornasari, D., Ceccherini, I., &
819 Bachetti, T. (2018). *Structural and functional differences in PHOX2B frameshift mutations*
820 *underlie isolated or syndromic congenital central hypoventilation syndrome*.
821 https://doi.org/10.1002/humu.23365

822 Drorbaugh, J. E., & Fenn, W. O. (1955). A barometric method for measuring ventilation in newborn
823 infants. *Pediatrics*, *16*(1), 81–87. https://doi.org/10.1542/peds.16.1.81

824 Dubreuil, V., Ramanantsoa, N., Trochet, D., Vaubourg, V., Amiel, J., Gallego, J., Brunet, J.-F., &
825 Goridis, C. (2008). A human mutation in Phox2b causes lack of CO2 chemosensitivity, fatal
826 central apnea, and specific loss of parafacial neurons. *Proceedings of the National Academy of*
827 *Sciences*, *105*(3), 1067–1072. https://doi.org/10.1073/pnas.0709115105

828 Dubreuil, V., Thoby-Brisson, M., Rallu, M., Persson, K., Pattyn, A., Birchmeier, C., Brunet, J.-F.,
829 Fortin, G., & Goridis, C. (2009). Defective Respiratory Rhythmogenesis and Loss of Central
830 Chemosensitivity in Phox2b Mutants Targeting Retrotrapezoid Nucleus Neurons. *Journal of*
831 *Neuroscience*, *29*(47), 14836–14846. https://doi.org/10.1523/JNEUROSCI.2623-09.2009

832 Durand, E., Dauger, S., Pattyn, A., Gaultier, C., Goridis, C., & Gallego, J. (2005). Sleep-disordered
833 breathing in newborn mice heterozygous for the transcription factor phox2b. *American Journal*

834 *of Respiratory and Critical Care Medicine*, *172*(2), 238–243.
835 https://doi.org/10.1164/rccm.200411-1528OC

836 Fan, Y., Huang, J., Duffourc, M., Kao, R. L., Ordway, G. A., Huang, R., & Zhu, M. Y. (2011).
837 Transcription factor Phox2 upregulates expression of norepinephrine transporter and
838 dopamine β-hydroxylase in adult rat brains. *Neuroscience*, *192*, 37–53.
839 https://doi.org/10.1016/j.neuroscience.2011.07.005

840 Gestreau, C., Heitzmann, D., Thomas, J., Dubreuil, V., Bandulik, S., Reichold, M., Bendahhou, S.,
841 Pierson, P., Sterner, C., Peyronnet-Roux, J., Benfriha, C., Tegtmeier, I., Ehnes, H., Georgieff, M.,
842 Lesage, F., Brunet, J.-F., Goridis, C., Warth, R., & Barhanin, J. (2010). Task2 potassium channels
843 set central respiratory CO2 and O2 sensitivity. *Proceedings of the National Academy of Sciences*,
844 *107*(5), 2325–2330. https://doi.org/10.1073/pnas.0910059107

845 Goridis, C., Dubreuil, V., Thoby-brisson, M., & Fortin, G. (2010). *Seminars in Cell & Developmental*
846 *Biology Phox2b , congenital central hypoventilation syndrome and the control of respiration*. *21*,
847 814–822. https://doi.org/10.1016/j.semcdb.2010.07.006

848 Gourine, A. V, Llaudet, E., Dale, N., & Spyer, K. M. (2005). *Behavioral/Systems/Cognitive Release of*
849 *ATP in the Ventral Medulla during Hypoxia in Rats: Role in Hypoxic Ventilatory Response*.
850 https://doi.org/10.1523/JNEUROSCI.3763-04.2005

851 Guyenet, P. G., Bayliss, D. A., Stornetta, R. L., Ludwig, M. G., Kumar, N. N., Shi, Y., Burke, P. G. R.,
852 Kanbar, R., Basting, T. M., Holloway, B. B., & Wenker, I. C. (2016). Proton detection and
853 breathing regulation by the retrotrapezoid nucleus. *Journal of Physiology*, *594*(6), 1529–1551.
854 https://doi.org/10.1113/JP271480

855 Guyenet, P. G., Stornetta, R. L., Souza, G. M. P. R., Abbott, S. B. G., Shi, Y., & Bayliss, D. A. (2019).
856 The Retrotrapezoid Nucleus: Central Chemoreceptor and Regulator of Breathing Automaticity.
857 *Trends in Neurosciences*, *42*(11), 807–824. https://doi.org/10.1016/J.TINS.2019.09.002

858 Harper, R. M., Kumar, R., Macey, P. M., Harper, R. K., & Ogren, J. A. (2015). Impaired neural
859 structure and function contributing to autonomic symptoms in congenital central
860 hypoventilation syndrome. *Frontiers in Neuroscience*, *9*(OCT), 415.
861 https://doi.org/10.3389/FNINS.2015.00415

862 Janes, T. A., Cardani, S., Saini, J. K., & Pagliardini, S. (2024b). Etonogestrel promotes respiratory
863 recovery in an in vivo rat model of central chemoreflex impairment. *Acta Physiologica*.
864 https://doi.org/10.1111/apha.14093

865 Kang, B. J., Chang, D. A., Mackay, D. D., West, G. H., Moreira, T. S., Takakura, A. C., Gwilt, J. M.,
866 Guyenet, P. G., & Stornetta, R. L. (2007). Central nervous system distribution of the
867 transcription factor Phox2b in the adult rat. *Journal of Comparative Neurology*, *503*(5), 627–
868 641. https://doi.org/10.1002/cne.21409

869 Kumar, N. N., Velic, A., Soliz, J., Shi, Y., Li, K., Wang, S., Weaver, J. L., Sen, J., Abbott, S. B. G.,
870 Lazarenko, R. M., Ludwig, M. G., Perez-Reyes, E., Mohebbi, N., Bettoni, C., Gassmann, M., Suply,
871 T., Seuwen, K., Guyenet, P. G., Wagner, C. A., & Bayliss, D. A. (2015). Regulation of breathing by
872 CO2 requires the proton-activated receptor GPR4 in retrotrapezoid nucleus neurons. *Science*,
873 *348*(6240), 1255–1260. https://doi.org/10.1126/science.aaa0922

Lighton, J. R. B. (2021). *MEASURING METABOLIC RATES : a manual for scientists.* https://global.oup.com/academic/product/measuring-metabolic-rates-9780198869320

Madani, A., Pitollat, G., Sizun, E., Cardoit, L., Ringot, M., Bourgeois, T., Ramanantsoa, N., Delclaux, C., Dauger, S., Thoby-Brisson, M., Gallego, J., & Matrot, B. (2021). Obstructive Apneas in a Mouse Model of Congenital Central Hypoventilation Syndrome. American journal of respiratory and critical care medicine, 204(10), 1200–1210. https://doi.org/10.1164/rccm.202104-0887OC.

Malheiros-Lima MR, Takakura AC, Moreira TS. Depletion of rostral ventrolateral medullary catecholaminergic neurons impairs the hypoxic ventilatory response in conscious rats. Neuroscience. 2017 May 20;351:1-14. doi: 10.1016/j.neuroscience.2017.03.031.

Marina, N., Abdala, A. P., Trapp, S., Li, A., Nattie, E. E., Hewinson, J., Smith, J. C., Paton, J. F. R., & Gourine, A. V. (2010). Essential Role of Phox2b-Expressing Ventrolateral Brainstem Neurons in the Chemosensory Control of Inspiration and Expiration. *Journal of Neuroscience*, *30*(37), 12466–12473. https://doi.org/10.1523/JNEUROSCI.3141-10.2010

Matera, I. (2004). PHOX2B mutations and polyalanine expansions correlate with the severity of the respiratory phenotype and associated symptoms in both congenital and late onset Central Hypoventilation syndrome. *Journal of Medical Genetics*, *41*(5), 373–380. https://doi.org/10.1136/jmg.2003.015412

Mcbride, J. L., Boudreau, R. L., Harper, S. Q., Staber, P. D., Monteys, A. M., Martins, I. S., Gilmore, B. L., Burstein, H., Peluso, R. W., Polisky, B., Carter, B. J., & Davidson, B. L. (2008). Artificial miRNAs mitigate shRNA-mediated toxicity in the brain: implications for the therapeutic development of RNAi. Proceedings of the National Academy of Sciences of the United States of America, 105(15), 5868–5873. https://doi.org/10.1073/pnas.0801775105

McCloy, R. A., Rogers, S., Caldon, C. E., Lorca, T., Castro, A., & Burgess, A. (2014). Partial inhibition of Cdk1 in G2 phase overrides the SAC and decouples mitotic events. *Cell Cycle*, *13*(9), 1400–1412. https://doi.org/10.4161/CC.28401/SUPPL_FILE/KCCY_A_10928401_SM0001.ZIP

Mortola, J. P., & Frappell, P. B. (1998). On the barometric method for measurements of ventilation, and its use in small animals.

Mortola, J. P., Matsuoka, T., Saiki, C., & Naso, L. (1994). RESPIRATION PHYSIOLOGY Metabolism and ventilation in hypoxic rats: effect of body mass. *Respiration Physiology*, *97*, 225–234.

Nagashimada, M., Ohta, H., Li, C., Nakao, K., Uesaka, T., Brunet, J. F., Amiel, J., Trochet, D., Wakayama, T., & Enomoto, H. (2012). Autonomic neurocristopathy-associated mutations in PHOX2B dysregulate Sox10 expression. *Journal of Clinical Investigation*, *122*(9), 3145–3158. https://doi.org/10.1172/JCI63401

Nattie, E. E., & Li, A. (1994). Retrotrapezoid nucleus lesions decrease phrenic activity and CO2 sensitivity in rats. *Respiration Physiology*, *97*(1), 63–77. https://doi.org/10.1016/0034-5687(94)90012-4

Nattie, E. E., & Li, A. (2002). Substance P-saporin lesion of neurons with NK1 receptors in one chemoreceptor site in rats decreases ventilation and chemosensitivity. *The Journal of Physiology*, *544*(2), 603–616. https://doi.org/10.1113/JPHYSIOL.2002.020032

913 Nobuta, H., Cilio, M. R., Danhaive, O., Tsai, H.-H., Tupal, S., Chang, S. M., Murnen, A., Kreitzer, F.,
914 Bravo, V., Czeisler, C., Gokozan, H. N., Gygli, P., Bush, S., Weese-Mayer, D. E., Conklin, B., Yee,
915 S.-P., Huang, E. J., Gray, P. A., Rowitch, D., & Otero, J. J. (2015). Dysregulation of locus coeruleus
916 development in congenital central hypoventilation syndrome. *Acta Neuropathologica*, *130*(2),
917 171–183. https://doi.org/10.1007/s00401-015-1441-0

918 Parodi, S., Di Zanni, E., Di Lascio, S., Bocca, P., Prigione, I., Fornasari, D., Pennuto, M., Bachetti, T.,
919 Ceccherini, I., Zanni, E. Di, Lascio, D., Bocca, P., Prigione, I., Fornasari, D., Pennuto, M., &
920 Bachetti, T. (2012). The E3 ubiquitin ligase TRIM11 mediates the degradation of congenital
921 central hypoventilation syndrome-associated polyalanine-expanded PHOX2B. *Journal of*
922 *Molecular Medicine*, *90*(9), 1025–1035. https://doi.org/10.1007/s00109-012-0868-1

923 Pattyn, A., Hirsch, M. R., Goridis, C., & Brunet, J. F. (2000). Control of hindbrain motor neuron
924 differentiation by the homeobox gene Phox2b. *Development (Cambridge, England)*, *127*(7),
925 1349–1358. https://doi.org/10.1242/DEV.127.7.1349

926 Pattyn, A., Morin, X., & Cremer, H. (1999). *The homeobox gene Phox2b is essential for the*
927 *development of autonomic neural crest derivatives*. *399*(May).

928 Pattyn, A., Morin, X., Cremer, H., Goridis, C., & Brunet, J. F. (1997). Expression and interactions of
929 the two closely related homeobox genes Phox2a and Phox2b during neurogenesis.
930 *Development (Cambridge, England)*, *124*(20), 4065–4075.
931 http://www.ncbi.nlm.nih.gov/pubmed/9374403

932 Paxinos, G., & Watson, C. *The rat brain in stereotaxic coordinates*, 2007

933 Pirone, L., Caldinelli, L., Di Lascio, S., Di Girolamo, R., Di Gaetano, S., Fornasari, D., Pollegioni, L.,
934 Benfante, R., & Pedone, E. (2019). Molecular insights into the role of the polyalanine region in
935 mediating PHOX2B aggregation. *FEBS Journal*, *286*(13), 2505–2521.
936 https://doi.org/10.1111/FEBS.14841

937 Ramanantsoa, N., Hirsch, M.-R., Thoby-Brisson, M., Dubreuil, V., Bouvier, J., Ruffault, P.-L., Matrot,
938 B., Fortin, G., Brunet, J.-F., Gallego, J., & Goridis, C. (2011). Breathing without CO2
939 Chemosensitivity in Conditional Phox2b Mutants. *Journal of Neuroscience*, *31*(36), 12880–
940 12888. https://doi.org/10.1523/JNEUROSCI.1721-11.2011

941 Seifert, E. L., Knowles, J., & Mortola, J. P. (2000). Continuous circadian measurements of
942 ventilation in behaving adult rats. *Respiration Physiology*, *120*, 179–183.
943 www.elsevier.com/locate/resphysiol

944 Shi, Y., Stornetta, R. L., Stornetta, D. S., Suna Onengut-Gumuscu, X., Farber, E. A., Turner, S. D.,
945 Guyenet, P. G., & Bayliss, D. A. (2017). *Neuromedin B Expression Defines the Mouse*
946 *Retrotrapezoid Nucleus*. https://doi.org/10.1523/JNEUROSCI.2055-17.2017

947 Shimokaze, T., Sasaki, A., Meguro, T., Hasegawa, H., Hiraku, Y., Yoshikawa, T., Kishikawa, Y., &
948 Hayasaka, K. (2015). Genotype-phenotype relationship in Japanese patients with congenital
949 central hypoventilation syndrome. *Journal of Human Genetics*, *60*(9), 473–477.
950 https://doi.org/10.1038/jhg.2015.65

Souza, G. M. P. R., Kanbar, R., Stornetta, D. S., Abbott, S. B. G., Stornetta, R. L., & Guyenet, P. G. (2018). Breathing regulation and blood gas homeostasis after near complete lesions of the retrotrapezoid nucleus in adult rats. *Journal of Physiology*, *596*(13), 2521–2545. https://doi.org/10.1113/JP275866

Souza, G. M. P. R., Stornetta, D. S., Shi, Y., Lim, E., Berry, F. E., Bayliss, D. A., & Abbott, S. B. G. (2023). Neuromedin B-Expressing Neurons in the Retrotrapezoid Nucleus Regulate Respiratory Homeostasis and Promote Stable Breathing in Adult Mice. *Journal of Neuroscience*, *43*(30), 5501–5520. https://doi.org/10.1523/JNEUROSCI.0386-23.2023

Stanke, M., Junghans, D., Geissen, M., Goridis, C., Ernsberger, U., & Rohrer, H. (1999). The Phox2 homeodomain proteins are sufficient to promote the development of sympathetic neurons. *Development*, *126*(18), 4087–4094. https://doi.org/10.1242/dev.00165

Stornetta, R. L., Moreira, T. S., Takakura, A. C., Kang, B. J., Chang, D. A., West, G. H., Mulkey, D. K., Bayliss, D. A., & Guyenet, P. G. (2006). *Expression of Phox2b by Brainstem Neurons Involved in Chemosensory Integration in the Adult Rat*. *26*(40), 10305–10314. https://doi.org/10.1523/JNEUROSCI.2917-06.2006

Takakura, A. C., Barna, B. F., Cruz, J. C., Colombari, E., & Moreira, T. S. (2014). Phox2b-expressing retrotrapezoid neurons and the integration of central and peripheral chemosensory control of breathing in conscious rats. *Experimental Physiology*, *99*(3). https://doi.org/10.1113/expphysiol.2013.076752

Takakura, A. C., Moreira, T. S., Stornetta, R. L., West, G. H., Gwilt, J. M., & Guyenet, P. G. (2008). Selective lesion of retrotrapezoid Phox2b-expressing neurons raises the apnoeic threshold in rats. *The Journal of Physiology*, *586*(Pt 12), 2975. https://doi.org/10.1113/JPHYSIOL.2008.153163

Tiveron, M. C., Hirsch, M. R., & Brunet, J. F. (1996). The expression pattern of the transcription factor Phox2 delineates synaptic pathways of the autonomic nervous system. *The Journal of Neuroscience : The Official Journal of the Society for Neuroscience*, *16*(23), 7649–7660. https://doi.org/10.1523/JNEUROSCI.16-23-07649.1996

Trang, H., Dehan, M., Beaufils, F., Zaccaria, I., Amiel, J., & Gaultier, C. (2005). The French Congenital Central Hypoventilation Syndrome Registry. *Chest*, *127*(1), 72–79. https://doi.org/10.1378/chest.127.1.72

Trochet, D., de Pontual, L., Estêvao, M. H., Mathieu, Y., Munnich, A., Feingold, J., Goridis, C., Lyonnet, S., & Amiel, J. (2008). Homozygous mutation of the PHOX2B gene in congenital central hypoventilation syndrome (Ondine's Curse). *Human Mutation*, *29*(5), 770–770. https://doi.org/10.1002/humu.20727

Trochet, D., Hong, S. J., Lim, J. K., Brunet, J. F., Munnich, A., Kim, K. S., Lyonnet, S., Goridis, C., & Amiel, J. (2005). Molecular consequences of PHOX2B missense, frameshift and alanine expansion mutations leading to autonomic dysfunction. *Human Molecular Genetics*, *14*(23), 3697–3708. https://doi.org/10.1093/hmg/ddi401

989 Van Gestel, M. A., Van Erp, S., Sanders, L. E., Brans, M. A. D., Luijendijk, M. C. M., Merkestein, M.,
990 Pasterkamp, R. J., & Adan, R. A. H. (2014). shRNA-induced saturation of the microRNA pathway
991 in the rat brain. *Gene Therapy*, *21*(2), 205–211. https://doi.org/10.1038/GT.2013.76

992 Van Limpt, V., Schramm, A., Lakeman, A., Van Sluis, P., Chan, A., Van Noesel, M., Baas, F., Caron,
993 H., Eggert, A., & Versteeg, R. (2004). The Phox2B homeobox gene is mutated in sporadic
994 neuroblastomas. *Oncogene*, *23*(57), 9280–9288. https://doi.org/10.1038/sj.onc.1208157

995 Weese-Mayer, D. E., Berry-Kravis, E. M., Zhou, L., Maher, B. S., Silvestri, J. M., Curran, M. E., &
996 Marazita, M. L. (2003). Idiopathic congenital central hypoventilation syndrome: Analysis of
997 genes pertinent to early autonomic nervous system embryologic development and
998 identification of mutations in PHOX2b. *American Journal of Medical Genetics*, *123A*(3), 267–
999 278. https://doi.org/10.1002/ajmg.a.20527

1000 Weese-Mayer, D. E., Rand, C. M., Zhou, A., Carroll, M. S., & Hunt, C. E. (2017). Congenital central
1001 hypoventilation syndrome: A bedside-to-bench success story for advancing early diagnosis and
1002 treatment and improved survival and quality of life. In *Pediatric Research* (Vol. 81, Issues 1–2).
1003 https://doi.org/10.1038/pr.2016.196

1004 Wickström, H. R., Berner, J., Holgert, H., Hökfelt, T., & Lagercrantz, H. (2004). Hypoxic response in
1005 newborn rat is attenuated by neurokinin-1 receptor blockade. *Respiratory Physiology and*
1006 *Neurobiology*, *140*(1), 19–31. https://doi.org/10.1016/j.resp.2004.01.008

1007 Wu, H., Su, Y., Hung, C., Hsieh, W., & Wu, K. (2009). *Interaction Between PHOX2B and CREBBP*
1008 *Mediates Synergistic Activation : Mechanistic Implications of PHOX2B Mutants Human*
1009 *Mutation*. https://doi.org/10.1002/humu.20929

1010 Zoccal, D. B., Furuya, W. I., Bassi, M., A Colombari, D. S., Colombari, E., Hildreth, C., & Putnam, R.
1011 W. (2014). *The nucleus of the solitary tract and the coordination of respiratory and sympathetic*
1012 *activities*. https://doi.org/10.3389/fphys.2014.00238

1013

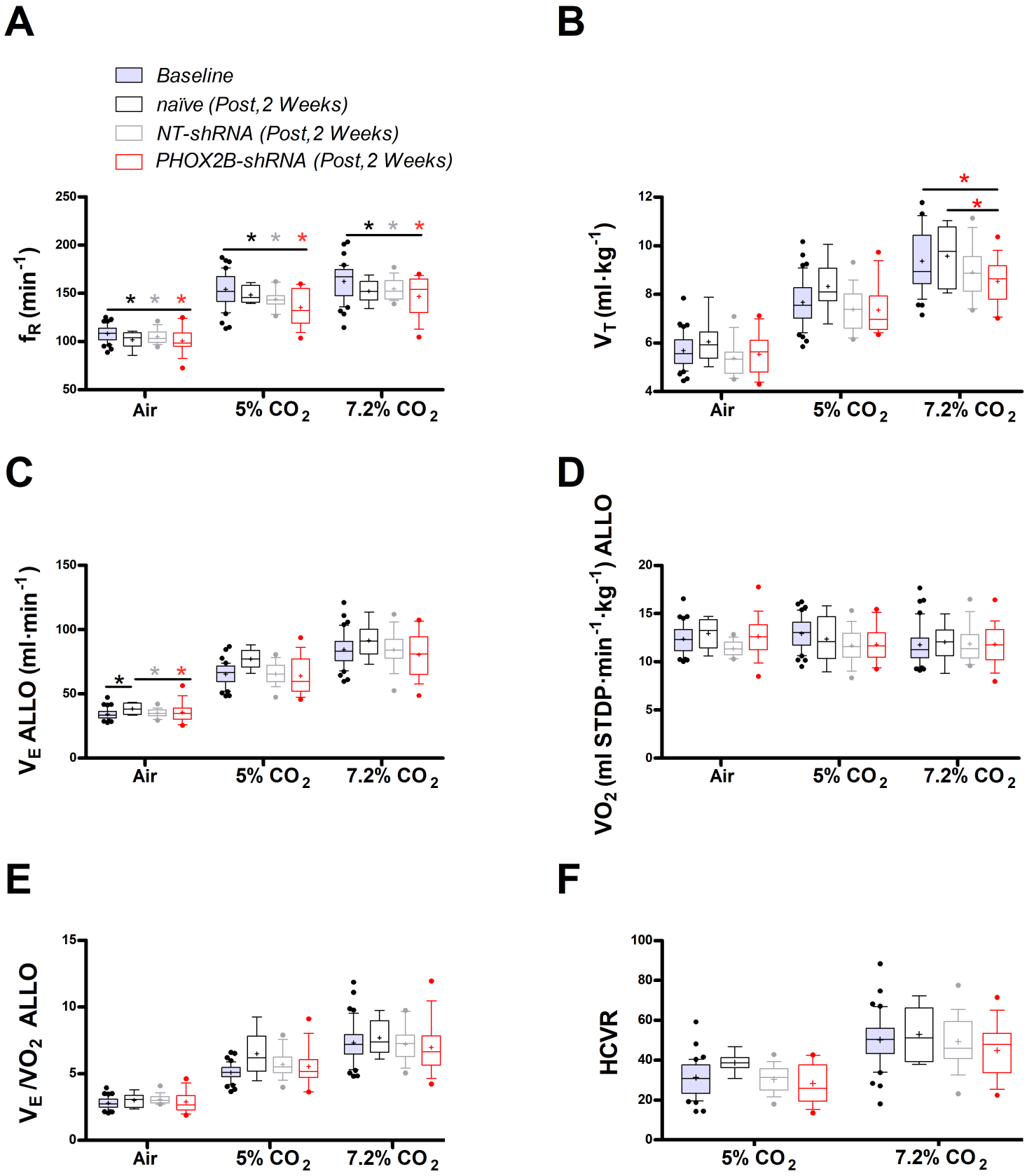
A
Baseline
naïve (Post,2 Weeks)
NT-shRNA (Post,2 Weeks)
PHOX2B-shRNA (Post,2 Weeks)
f_R (min^{-1})
250
200
150
100
50
Air
5% CO_2
7.2% CO_2
B
V_T (ml·kg^{-1})
12
10
8
6
4
Air
5% CO_2
7.2% CO_2
C
V_E ALLO (ml·min^{-1})
150
100
50
0
Air
5% CO_2
7.2% CO_2
D
VO_2 (ml STDP·min^{-1}·kg^{-1}) ALLO
20
15
10
5
0
Air
5% CO_2
7.2% CO_2
E
V_E /VO_2 ALLO
15
10
5
0
Air
5% CO_2
7.2% CO_2
F
HCVR
100
80
60
40
20
0
5% CO_2
7.2% CO_2

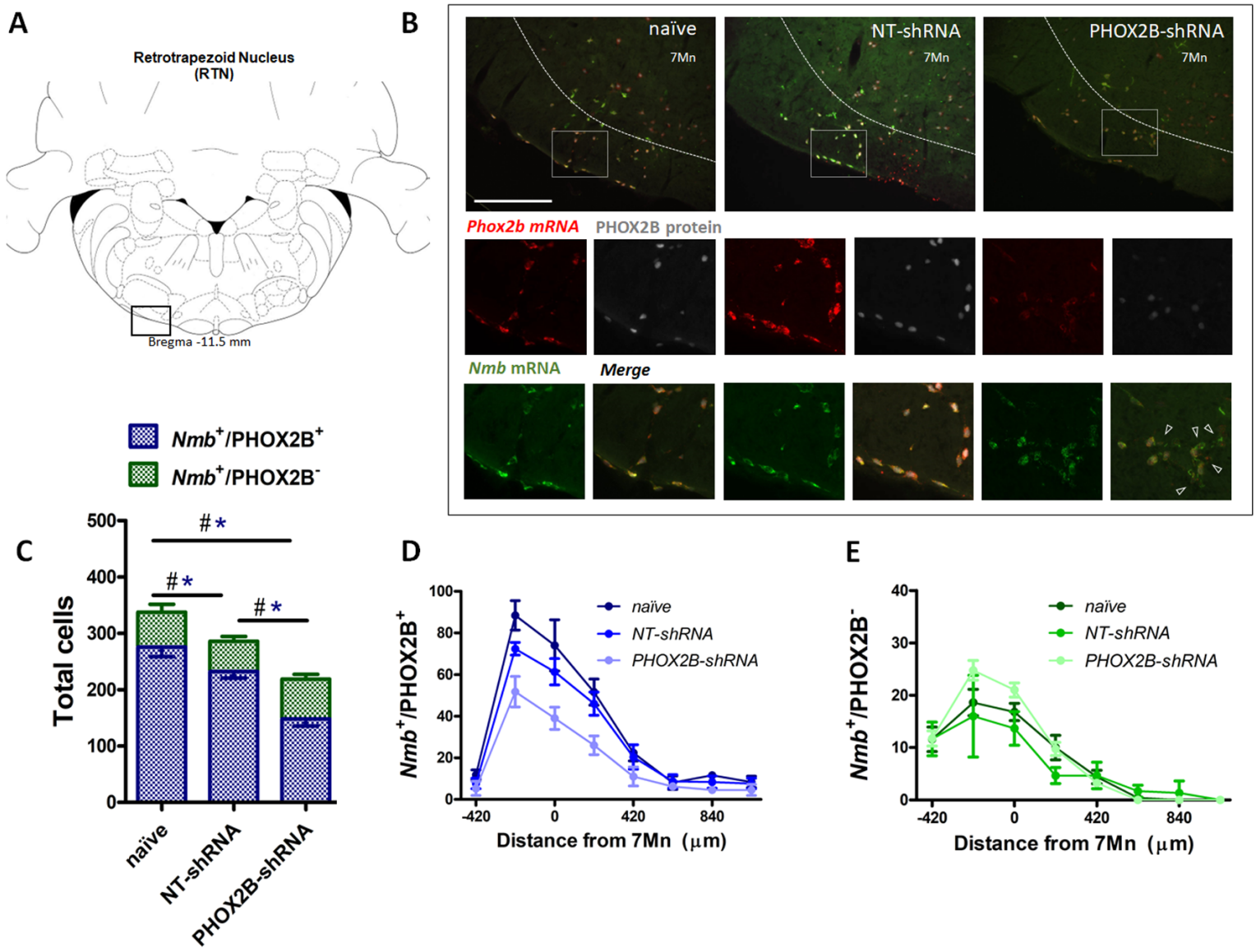
A
Retrotrapezoid Nucleus
(RTN)
Bregma -11.5 mm
B
naïve
7Mn
NT-shRNA
7Mn
PHOX2B-shRNA
7Mn
Phox2b mRNA
PHOX2B protein
Nmb mRNA
Merge
Nmb+/PHOX2B+
Nmb+/PHOX2B-
C
Total cells
500
400
300
200
100
0
#*
#*
#*
naïve
NT-shRNA
PHOX2B-shRNA
D
Nmb+/PHOX2B+
100
80
60
40
20
0
naïve
NT-shRNA
PHOX2B-shRNA
-420
0
420
840
Distance from 7Mn (μm)
E
Nmb+/PHOX2B-
40
30
20
10
0
naïve
NT-shRNA
PHOX2B-shRNA
-420
0
420
840
Distance from 7Mn (μm)

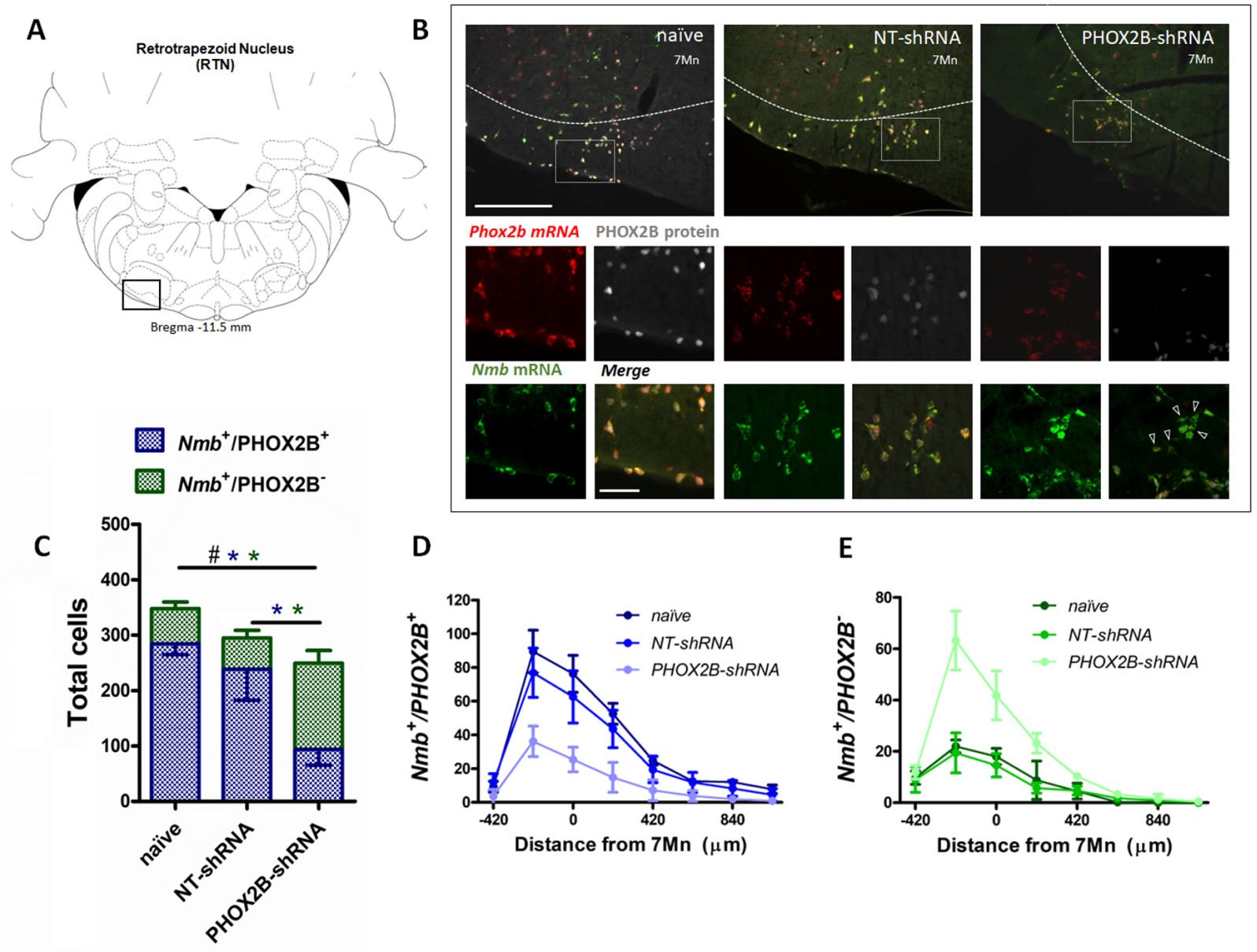
A
Retrotrapezoid Nucleus
(RTN)
Bregma -11.5 mm
B
naïve
7Mn
NT-shRNA
7Mn
PHOX2B-shRNA
7Mn
Phox2b mRNA
PHOX2B protein
Nmb mRNA
Merge
Nmb+/PHOX2B+
Nmb+/PHOX2B-
C
Total cells
500
400
300
200
100
0
* *
* *
naïve
NT-shRNA
PHOX2B-shRNA
D
Nmb+/PHOX2B+
120
100
80
60
40
20
0
naïve
NT-shRNA
PHOX2B-shRNA
-420
0
420
840
Distance from 7Mn (μm)
E
Nmb+/PHOX2B-
80
60
40
20
0
naïve
NT-shRNA
PHOX2B-shRNA
-420
0
420
840
Distance from 7Mn (μm)

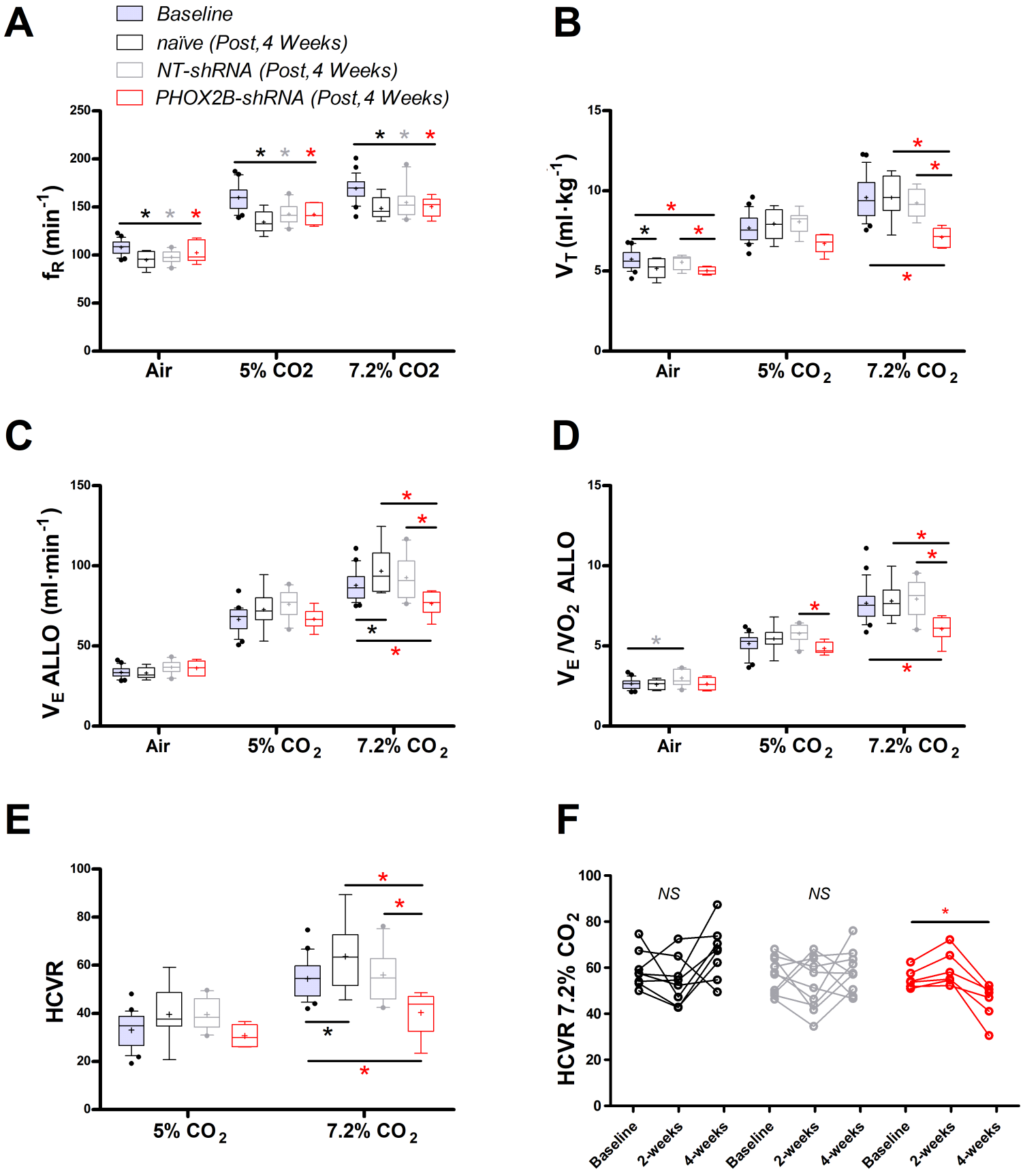
A
Baseline
naïve (Post, 4 Weeks)
NT-shRNA (Post, 4 Weeks)
PHOX2B-shRNA (Post, 4 Weeks)
f_R (min^{-1})
Air
5% CO2
7.2% CO2
B
V_T (ml·kg^{-1})
Air
5% CO_2
7.2% CO_2
C
V_E ALLO (ml·min^{-1})
Air
5% CO_2
7.2% CO_2
D
V_E /VO_2 ALLO
Air
5% CO_2
7.2% CO_2
E
HCVR
5% CO_2
7.2% CO_2
F
HCVR 7.2% CO_2
NS
NS
Baseline
2-weeks
4-weeks
Baseline
2-weeks
4-weeks
Baseline
2-weeks
4-weeks

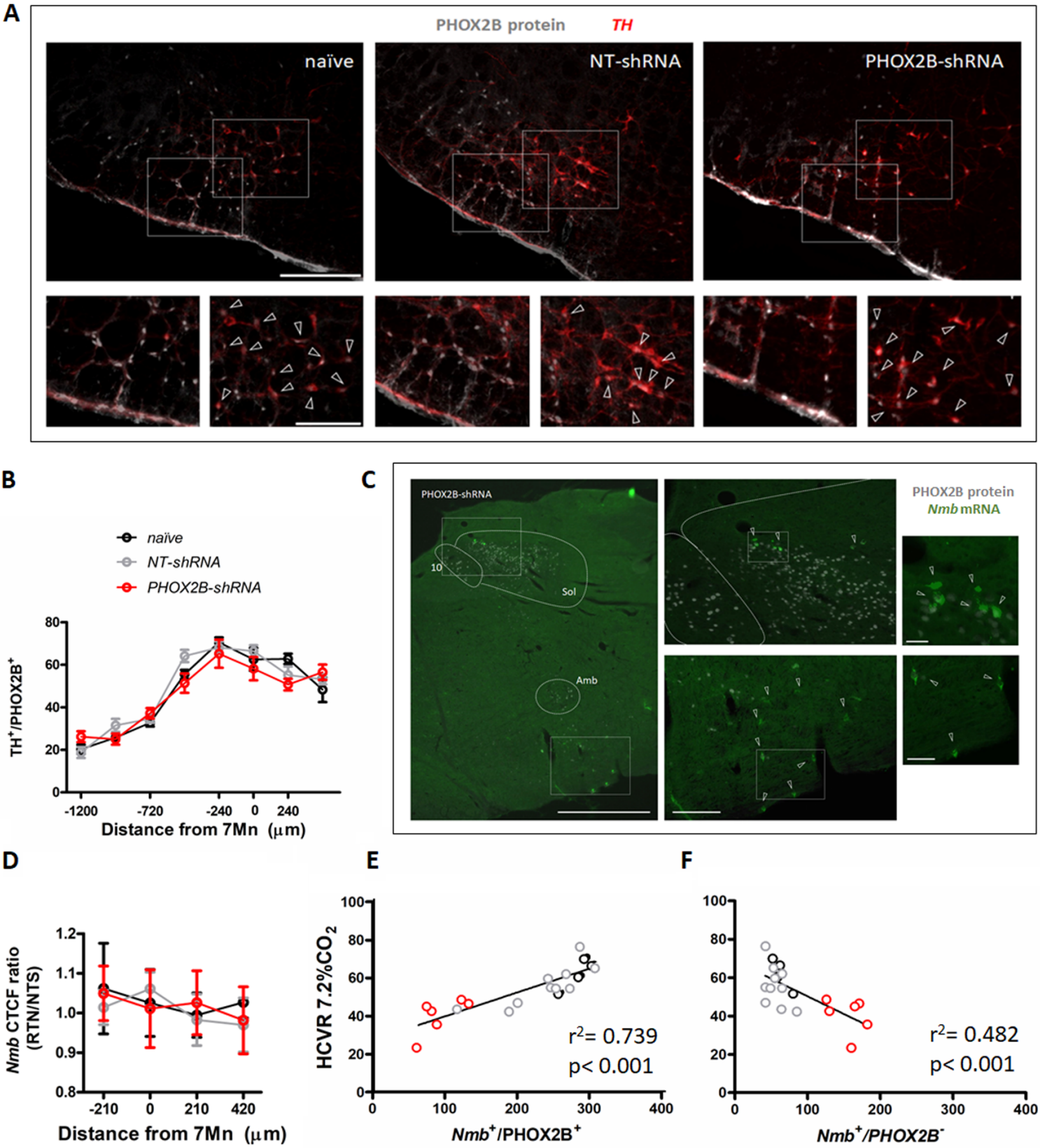
A
PHOX2B protein
TH
naïve
NT-shRNA
PHOX2B-shRNA
B
naïve
NT-shRNA
PHOX2B-shRNA
TH+/PHOX2B+
Distance from 7Mn (μm)
C
PHOX2B-shRNA
10
Sol
Amb
PHOX2B protein
Nmb mRNA
D
Nmb CTCF ratio (RTN/NTS)
Distance from 7Mn (μm)
E
HCVR 7.2%CO2
r2= 0.739
p< 0.001
Nmb+/PHOX2B+
F
r2= 0.482
p< 0.001
Nmb+/PHOX2B-

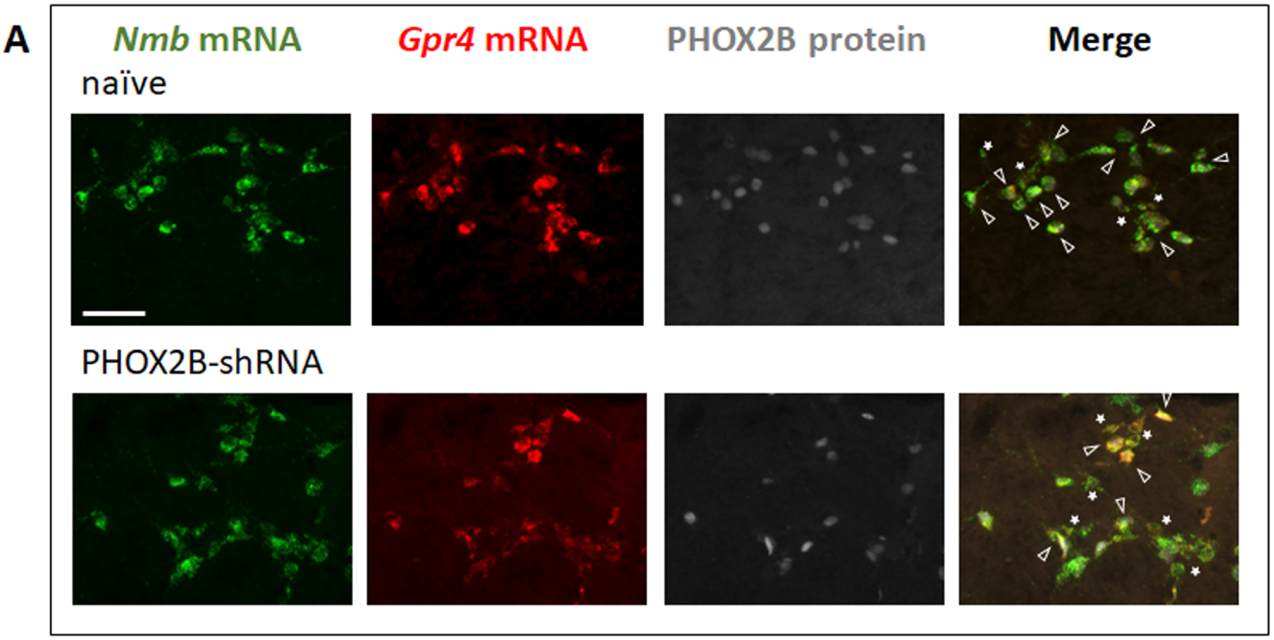
A
Nmb mRNA
Gpr4 mRNA
PHOX2B protein
Merge
naïve
PHOX2B-shRNA

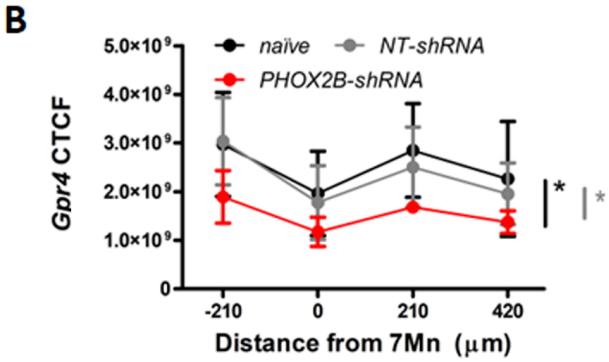
B
naïve
NT-shRNA
PHOX2B-shRNA
Gpr4 CTCF
5.0×10⁹
4.0×10⁹
3.0×10⁹
2.0×10⁹
1.0×10⁹
0
-210
0
210
420
Distance from 7Mn (μm)
*
*

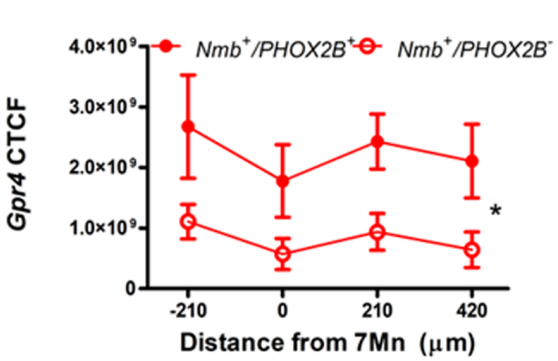
C
Nmb⁺/PHOX2B⁺
Nmb⁺/PHOX2B⁻
Gpr4 CTCF
4.0×10⁹
3.0×10⁹
2.0×10⁹
1.0×10⁹
0
-210
0
210
420
Distance from 7Mn (μm)
*

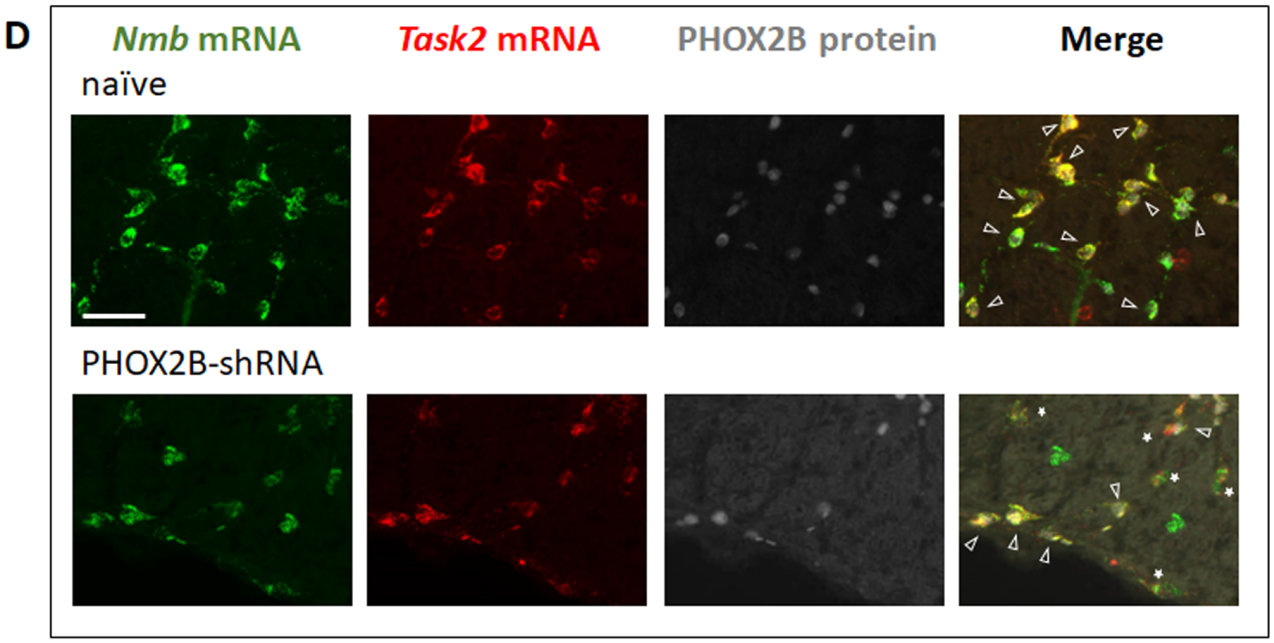
D
Nmb mRNA
Task2 mRNA
PHOX2B protein
Merge
naïve
PHOX2B-shRNA

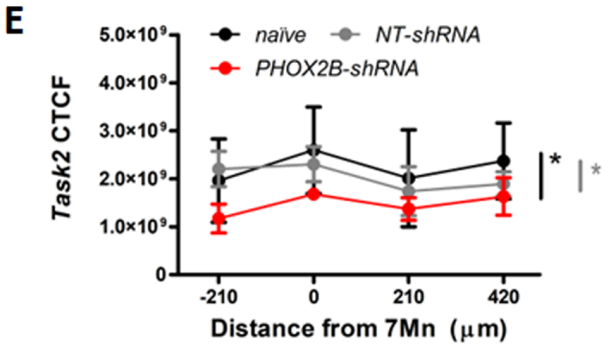
E
naïve
NT-shRNA
PHOX2B-shRNA
Task2 CTCF
5.0×10⁹
4.0×10⁹
3.0×10⁹
2.0×10⁹
1.0×10⁹
0
-210
0
210
420
Distance from 7Mn (μm)
*
*

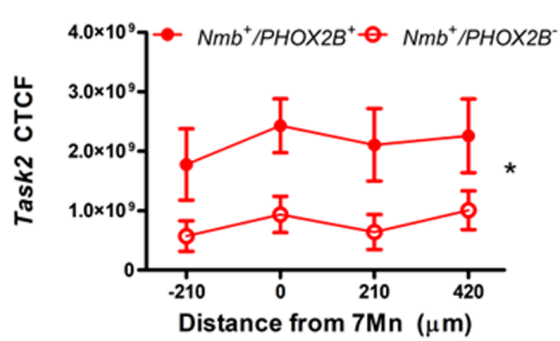
F
Nmb⁺/PHOX2B⁺
Nmb⁺/PHOX2B⁻
Task2 CTCF
4.0×10⁹
3.0×10⁹
2.0×10⁹
1.0×10⁹
0
-210
0
210
420
Distance from 7Mn (μm)
*